Sensors and Actuators Reports 2 (2020) 100020

Contents lists available at ScienceDirect

Sensors and Actuators Reports

journal homepage: www.elsevier.com/locate/snr

Sensing guanine and its derivatives: From molecular recognition to applications

Yuqing Li [a], Juewen Liu [a,b,*]

[a] Department of Chemistry, Waterloo Institute for Nanotechnology, University of Waterloo, Waterloo, Ontario N2L 3G1, Canada
[b] Centre for Eye and Vision Research, 17W Hong Kong Science Park, Hong Kong

ARTICLE INFO

Keywords:
Aptamers
Fluorescence
Biosensors
GTP
Guanosine

ABSTRACT

Guanine plays an indispensable role in building nucleic acids, and its derivatives take part in various cellular functions such as regulating biological reactions and signal transduction. Monitoring the levels of guanine and its derivatives is critical for understanding their biological roles and related diseases. Aside from traditional chromatography-based methods, majority of the current detections were based on electrochemistry and the oxidation activity of guanine, for which guanine and adenine often had a similar response. Over the last 30 years, various new sensing strategies have been developed. To provide researchers with more options for specific sensing of guanine and its derivatives, herein we review molecular recognition strategies based on nucleic acids, proteins, small organic molecules, molecularly imprinted polymers to nanomaterials. The mechanism of each molecular recognition strategy is discussed. Based on these target recognition molecules, we also critically review representative fluorescent and electrochemical sensors for guanine-related analytes from an application point of view, and provide readers with our perspectives to further grow this direction.

1. Introduction

Guanine is one of the four nucleobases of DNA carrying genetic information, and its derivatives play key regulatory roles in cellular functions. For example, extracellular guanosine and guanosine monophosphate (GMP) modulate the activities of neural cells, whereas intracellular GDP and GTP work with G-proteins to control transmembrane signal transduction [1]. Abnormal levels of guanine and its derivatives can lead to serious problems [2–4]. For instance, a low GMP level results in neurodegenerative brainstem disorders [5], a high concentration of guanosine excretion is related to carcinoma [6], and an elevated level of 8-oxoguanine reflects reduced DNA-repair capacity and an increased risk of cancer [7]. Therefore, monitoring the concentration of guanine and its derivatives is critical for understanding their biological roles and related disease diagnosis.

Conventional methods for analyzing guanine-contained compounds rely heavily on chromatographic methods, such as high-performance liquid chromatography (HPLC) [8, 9], gas chromatography [10], mass spectrometry [11, 12], and microdialysis [13]. They are highly sensitive and selective, but time-consuming, expensive, or difficult to operate. In addition, in situ detection is difficult, and samples need to be extracted and processed before measurement.

Therefore, alternative biosensing strategies have been explored to meet this analytical challenge. Riboswitches and antibodies are naturally found ligands that can specifically bind guanine and derivates [14, 15]. Due to their complexity and low stability, systematic evolution of ligands by exponential enrichment (SELEX) was employed to generate aptamers [16–20]. DNA aptamers are more robust and preferred than RNA aptamers in analytical applications. On the other hand, however, the specificity of SELEX-derived aptamers are sometimes insufficient [21]. In addition, non-SELEX DNA-based strategies were also developed in recent years, such as using abasic site DNA complexes [22, 23], vacancy-bearing G-quadruplexes [24], and base excised DNA [25, 26]. Aside from nucleic acid based ligands, some proteins, small organic molecules and molecularly imprinted polymers can also specifically interact with guanine containing molecules [27–30], whereas other sensing strategies take advantage of easy oxidation of guanine [31].

Given the development in guanine recognition and sensing, we herein review on this topic and the related target molecules are listed in Fig. 1. The mechanisms of molecular recognition are discussed and compared, and some analytical applications are briefly covered. We critically reviewed the field and also provided our own opinion.

2. SELEX-derived aptamers and DNAzymes

2.1. RNA aptamer for xanthine/guanine

A guanine becomes a xanthine when its amine group is replaced by an oxo (Fig. 1A and B). Xanthine can be generated by guanine

* Corresponding author at: Department of Chemistry, Waterloo Institute for Nanotechnology, University of Waterloo, Waterloo, Ontario N2L 3G1, Canada.
E-mail address: liujw@uwaterloo.ca (J. Liu).

https://doi.org/10.1016/j.snr.2020.100020
Received 29 August 2020; Revised 17 September 2020; Accepted 20 September 2020
Available online 28 September 2020

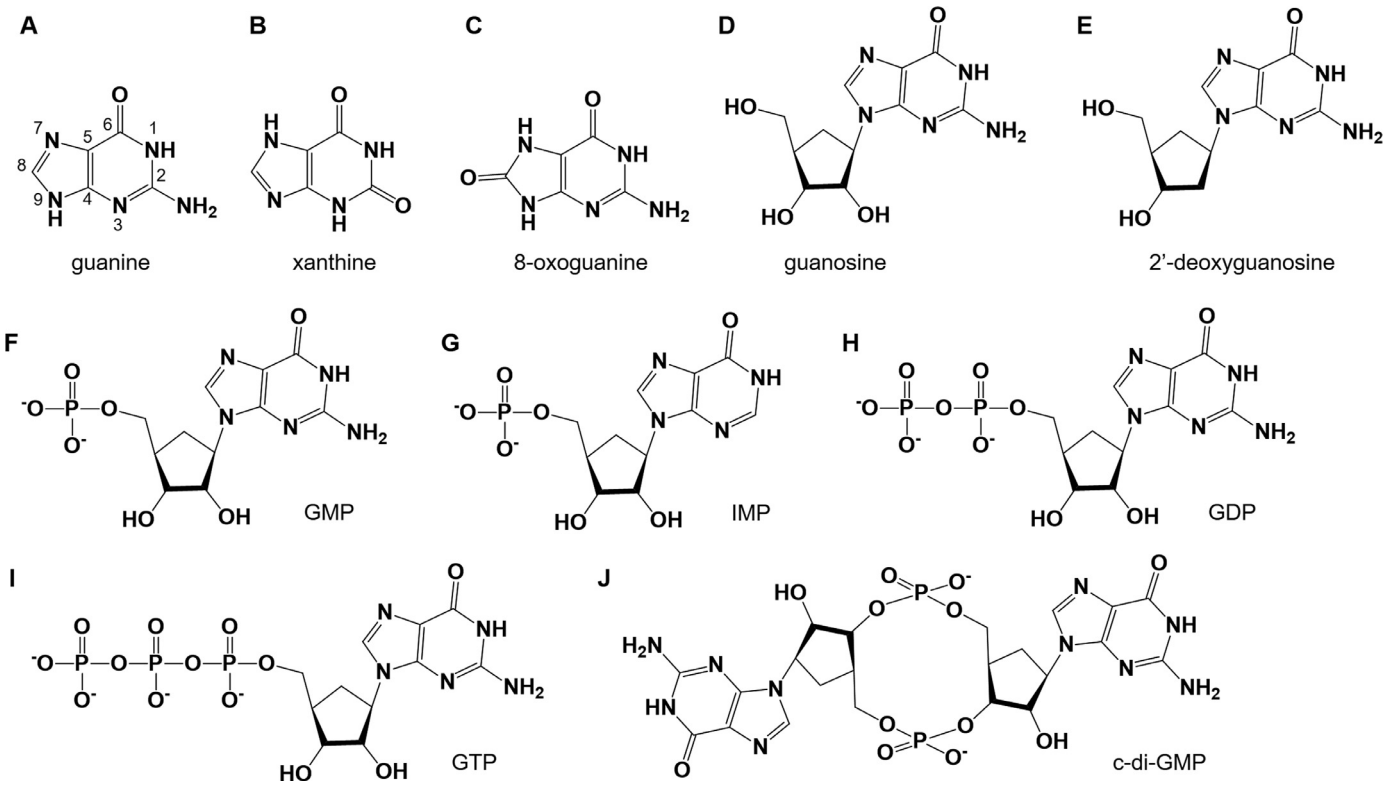

Fig. 1. Chemical structures of guanine and its derivatives reviewed including (A) guanine, (B) xanthine, (C) 8-oxoguanine, (D) guanosine, (E) 2′-deoxyguanosine, (F) GMP, (G) inosine monophosphate (IMP), (H) GDP, (I) GTP and (J) c-di-GMP.

deaminase. With xanthine oxidase, it is further converted to uric acid, and a high concentration of uric acid can lead to gout and calculi in kidneys [32]. In 1998, Yokoyama et al. selected the first xanthine/guanine RNA aptamer [33]. Through immobilizing xanthine on its C8 position to agarose (Fig. 2A), the xanthine binding sequences were enriched. Fig. 2B shows the optimal 32-mer aptamer exhibiting a K_d of 4.1 ± 0.6 μM xanthine and 1.8 ± 0.4 μM guanine. Hypoxanthine and 3-methylxanthine can also bind with similar affinities of 2.1 ± 0.5 μM and 2.7 ± 0.4 μM, respectively. Interestingly, the binding of guanosine was much weaker (K_d 140 ± 10 μM), while other nucleobases like adenine, cytosine and uracil can hardly bind. From the structure of these analogues, the N1H, N7 and O6 positions are important for aptamer-ligand interactions.

2.2. RNA aptamer for guanosine

A guanosine binding RNA aptamer was selected by Connell and Yarus [34]. They modified the phosphate of GDP on an agarose column to ensure that the guanosine part could fully interact with the library. CMP, AMP, and GMP were successively applied to wash the column but only the last elution containing the GMP-associated strands was collected and amplified. The best aptamer (Fig. 2D) could bind guanosine and guanine nucleotides with a similar affinity (K_d 32 ± 2 μM guanosine), yet it had no affinity for AMP, UMP or CMP. The C6O (very crucial), N1H, N2H and N7 positions were found important for ligand recognition.

To understand the effect of ligand change on binding specificity of the RNA aptamer, the authors further selected an aptamer that can recognize both arginine and guanosine. The library was first applied to an arginine affinity chromatography and eluted by L-arginine, and then transferred to a GDP-agarose column and eluted by GMP. Consequently, an arginine-guanosine aptamer was obtained (Fig. 2E), showing a K_d of 205 ± 1 μM guanosine and 4.1 ± 0.4 mM arginine. Through comparing the secondary structures of these two aptamers, a consensus domain (Fig. 2D and E, in red) was identified, indicating its importance in recognizing the guanosine.

2.3. RNA and DNA aptamers for GTP

Since many aptamers were found to have at least one internal stem-loop structure [35–38], Davis and Szostak studied whether introducing such a stem-loop structure would be helpful for selecting high-affinity aptamers [39]. To test this idea, their RNA library was designed to have a central 12-nt sequence forming a 4-bp stem loop, flanked by two random regions. After the selection, seven aptamer candidates were identified with K_d's from 25 nM to 500 μM. Among them, a sequence named 9–4 showed the highest affinity (K_d = 25 nM), and the initially designed stem-loop structure was indeed present in the aptamers (the red region of Fig. 2C).

Later, the authors characterized a variant of the 9–4 aptamer, and found that the variant contained three stems and two internal bulge-loops, together contributing to the tight GTP affinity [40]. Based on this, they proposed an idea that more complex structures were required to bind GTP with improved affinity. To test this idea, the authors performed a new selection and found that the simple stem-loop bearing aptamers only showed weaker binding (K_d from 250 nM to 900 nM), internal bulge-loop aptamers had K_d of 30 nM, and the most complex aptamers with three stems and two internal bulge-loops had the tightest affinity from 9 nM to 17 nM GTP. However, tightest affinity did not mean highest specificity [41]. The 9-4 aptamer can even bind 1-methylguanosine, 6-thio-GTP and 7-methyl-GTP, while some aptamers with weaker affinities for GTP had better selectivity.

The above aptamer selections were performed between 2002 and 2004, all using RNA libraries. Later, interest on DNA aptamers caught up for their higher stability and lower cost. Instead of immobilizing target ligands, in 2005, Nutiu and Li selected a new GTP binding DNA

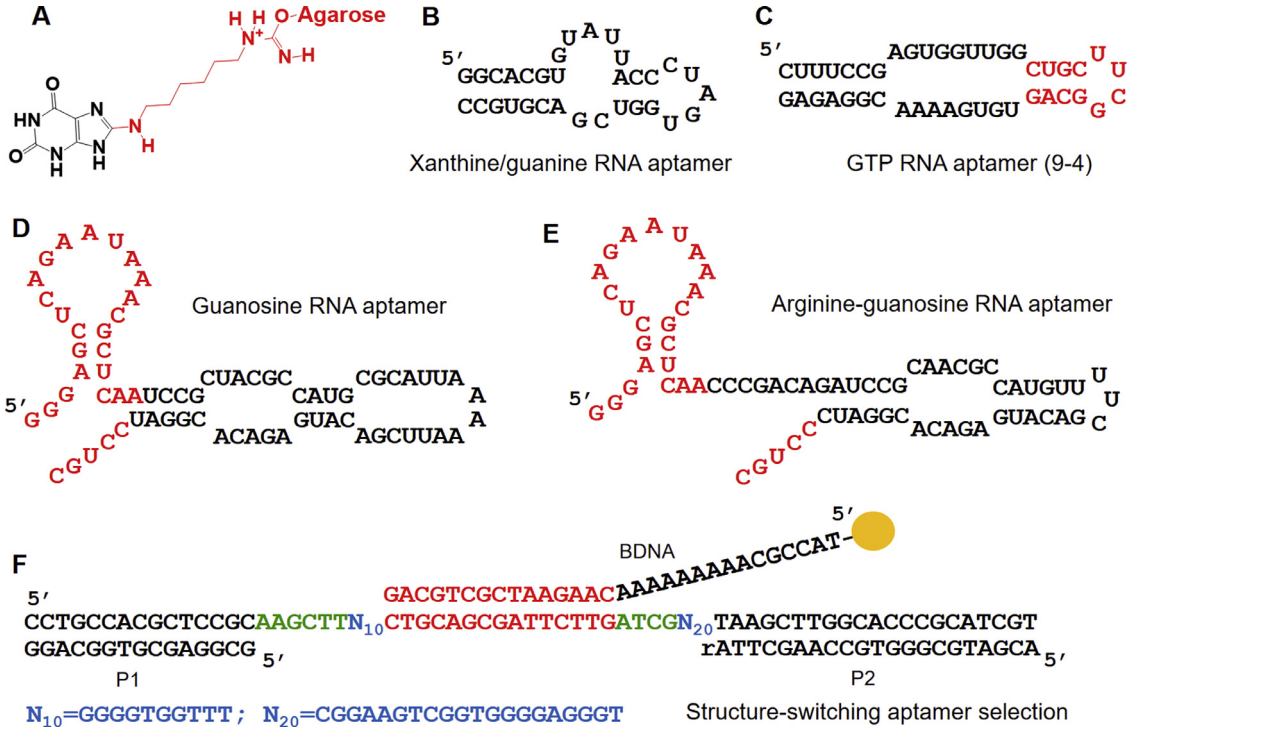

Fig. 2. (A) Immobilization of xanthine on agarose through its C8 position. The secondary structures of the (B) xanthine/guanine RNA aptamer, (C) GTP RNA aptamer (9-4), (D) guanosine RNA aptamer and (E) arginine-guanosine RNA aptamer. (F) The library design for selecting structure-switching aptamers. (For interpretation of the references to color in this figure, the reader is referred to the web version of this article.)

aptamer by immobilizing the DNA library as shown in Fig. 2F [42]. The red domain was hybridized with a biotinylated complementary strand at its 5′-end (BDNA), enabling the library to be attached on the avidin-coated beads. The flanked blue parts were the randomized region of the library. Adding GTP would result in the release of some sequences that can bind GTP and experience a structure switching process. By having this conformational change, when a fluorophore and a quencher were attached to the 5′-P1 and 3′-BDNA, the binding of GTP can synchronize a fluorescence signal increase.

2.4. DNAzymes for GTP

DNAzymes, also referred to as catalytic DNA or deoxyribozymes, are DNA oligonucleotides having catalytic activities. DNAzymes are so far only obtained by in vitro selections [43–47], and they are known for the detection of various metal ions [48–50]. The first GTP/Mn^{2+}-dependent DNAzyme for DNA phosphorylation was reported by Li et al. in 2002, and Mn^{2+} acted as cofactor in this case [51]. The mechanism of the selection is described in Fig. 3A, in which the 5′-OH in DNA

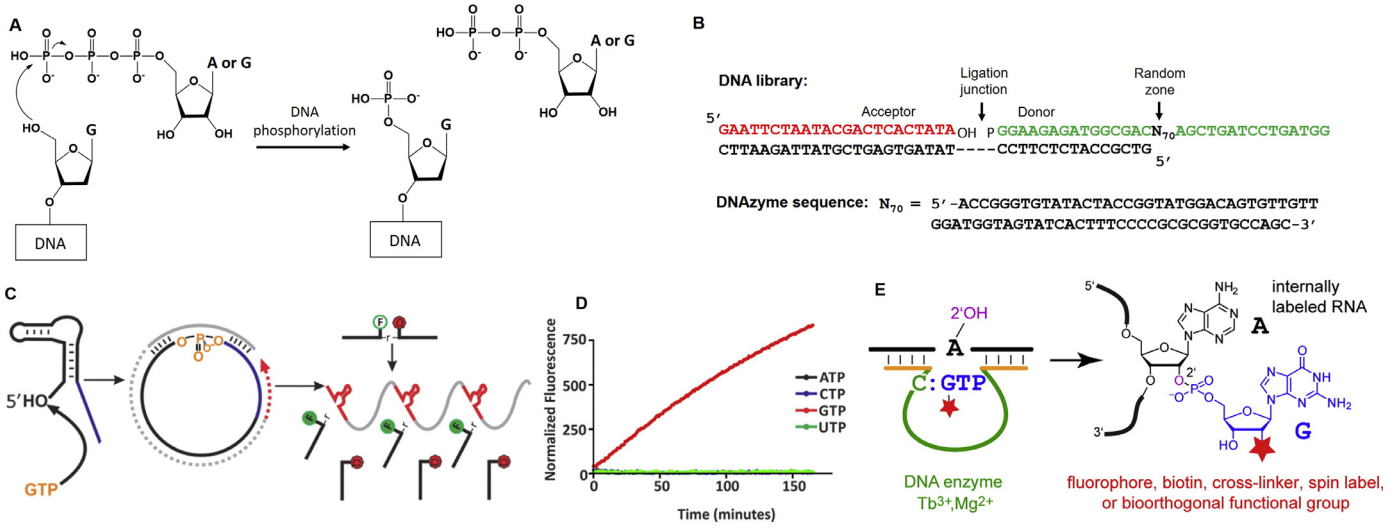

Fig. 3. (A) Reaction scheme for a self-phosphorylating DNAzyme. (B) DNA library design and the optimal sequence for the selected DNAzyme to ligate 5′-OH and the γ-phosphate in GTP. (C) Scheme for RCA-based highly sensitive GTP-detection. (D) GTP specificity of the DNAzyme-based sensor in (C). Reproduced with permission [52]. Copyright 2013, American Chemical Society. (E) Scheme for a DNAzyme to ligate the 2′-OH and α-phosphate in GTP. Reproduced with permission [55]. Copyright 2014, American Chemical Society. (For interpretation of the references to color in this figure, the reader is referred to the web version of this article.)

phosphorylated with the γ-phosphate in a GTP can further ligate with another DNA to form a longer strand. Based on this, their library was designed in Fig. 3B, where the red and green domains are the acceptor and donor, contributing 5′-OH and phosphate for the ligation reaction, respectively. Only the ligated strands were collected, and an optimal sequence is in the lower panel of Fig. 3B. The K_m for Mn^{2+} and GTP were 5.6 mM and 0.55 mM, respectively, and the K_{cat} was at 0.8 min^{-1}. Apart from the GTP, ATP can also be the other source of activated phosphate, and this DNAzyme can hardly distinguish GTP from the ATP (only 0.7-fold selectivity based on K_m(GTP)/K_m(ATP)).

To improve the sensitivity and thereby boost the detection limit, signal amplification processes were involved in several follow-up works [52, 53]. For example, Li et al. developed this DNAzyme into a GTP-sensor by introducing a rolling circle amplification (RCA) reaction (Fig. 3C) [52]. The 3′-end of the DNAzyme (in black) was extended to contain the antisense sequence (in blue) of an RNA-cleaving DNAzyme (named MgZ, in red). In the presence of GTP, the 5′-end of the strand was phosphorylated and then circularized to template the RCA process in the presence of Φ29 DNA polymerase. This RCA reaction can produce long, repetitive sequence of more than 10 kilobases. In the next step, a fluorophore and quencher labeled substrate was added to produce increased fluorescence after cleavage [54]. Interestingly, the signal of ATP became much less in this system (Fig. 3D). As low as 25 nM GTP can be detected even in the presence of 1 mM ATP.

In addition to DNA phosphorylation on the 5′-OH, the 2′-OH could also react with the α-phosphate in GTP, as reported by the Höbartner group in a new selection [55]. Fig. 3E describes this reaction, in which the substrate was attached through a 2′,5′-phosphodiester bond, and a pyrophosphate (derived from the β- and γ-phosphate of GTP) was generated as a leaving group. The DNAzyme can be used for RNA labeling. The red star (shown in Fig. 3E) can be different moieties, such as fluorophore (e.g. Cy3 and Cy5) and biotin. The use of this reaction for the detection of GTP has not yet been demonstrated.

2.5. Detection of intracellular GTP

The GTP RNA aptamer (Class I, Fig. 2C) was used for monitoring intracellular GTP by Li, Lin and coworkers. They adsorbed the Cy5-labeled GTP aptamer and a FAM-labeled ATP aptamer on graphene oxide nanosheets (GO-nS). The GO-nS carried the aptamer probes into cells and also to quench their fluorescence. Upon binding to the target GTP and ATP, the aptamers desorbed with enhanced fluorescence (Fig. 4) [56, 57]. In buffer, when incubating the sensor with 10 μM–2 mM GTP, the fluorescence of aptamer-Cy5 recovered linearly, and the characterization of the ATP sensor was previously reported [58]. In the confocal fluorescence micrograph, the green and red fluorescence represented cellular ATP and GTP, respectively. It is interesting to note that these two fluorescence signals were on completely different locations, suggesting the distribution of ATP and GTP in living cells (the right panel, Fig. 4).

3. Riboswitches

Riboswitches are mainly found in the 5′ untranslated regions (UTRs) of mRNAs in bacterial cells and can specifically recognize certain metabolites, including adenine and guanine. This recognition can subsequently activate or repress gene expression based on the concentration of target metabolites [59–62].

3.1. Riboswitch for guanine

Wöhnert et al. characterized the guanine riboswitch in the *xpt-pbuX*-mRNA (Fig. 5A) [63]. Its C_{74} residue is highly conserved and any mutations to it deprived its affinity for guanine. This mRNA domain has a very tight K_d of 5 nM guanine, whereas it binds adenine at least 100,000-fold weaker. Interestingly, in the *ydhL*-mRNA, the binding region of adenine is highly similar to that of guanine, except that the C_{74} changes to U_{74}. Mutation of this U to C enables guanine to re-fit into the *ydhL*-mRNA but not adenine anymore [64]. The guanine riboswitch in the *xpt-pbuX*-mRNA has not yet been applied for analytical applications [65].

3.2. Riboswitch for 2′-deoxyguanosine

Breaker and coworkers identified several guanine riboswitch variants from *Mesoplasma florum*, and found that one of them was highly selective for binding 2′-deoxyguanosine (2′-dG) [67]. It was named the I-A aptamer (Fig. 5B), with 39-nucleotide differences relative to the *xpt* mRNA for guanine. The original C_{74} position was re-numbered to C_{80}, but the cytosine was still highly conserved for interacting with 2′-dG

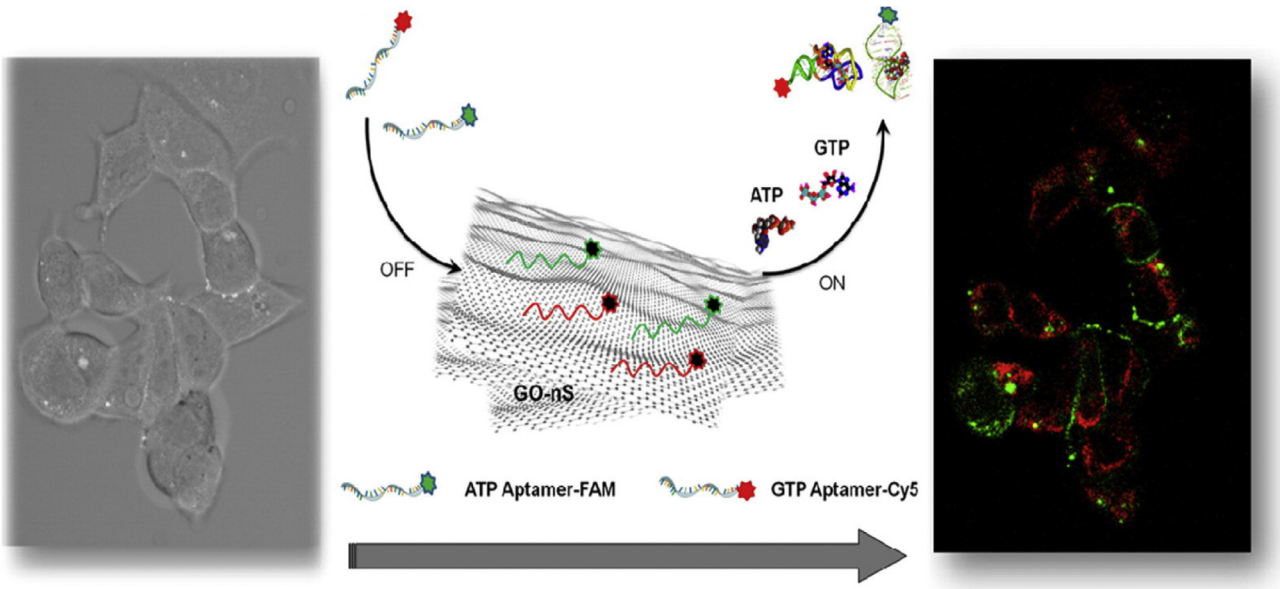

Fig. 4. Schematic illustration of the multiple sensing platform based on Cy5-GTP RNA aptamer and FAM-ATP DNA aptamer as reporters and GO-nS as a carrier. The cells were lighted up in the presence of GTP and ATP. Reproduced with permission [56]. Copyright 2013, American Chemical Society.

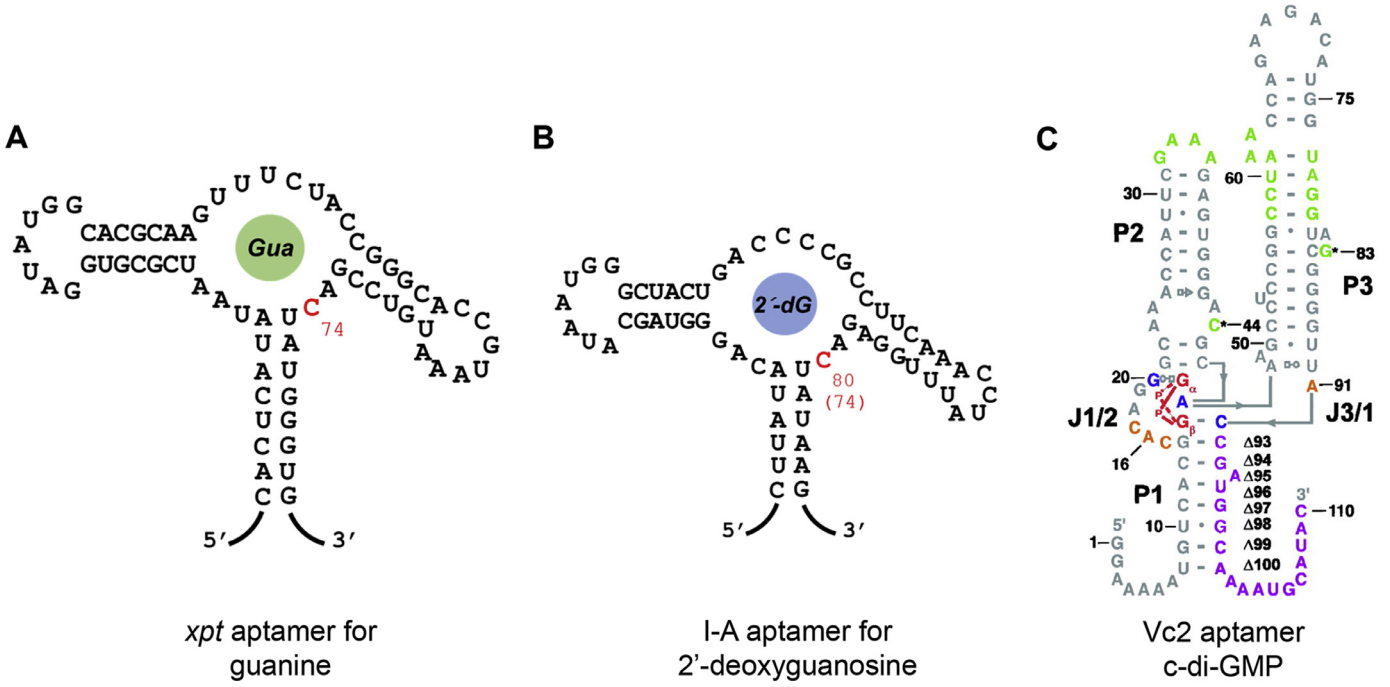

Fig. 5. The secondary structures of the (A) *xpt* aptamer for guanine, (B) I-A aptamer for 2′-deoxyguanosine, and (C) Vc2 aptamer for c-di-GMP. Reproduced with permission from reference [66]. Copyright 2010, American Chemical Society.

through a Watson-Crick base pair. The apparat K_d was determined to be around 80 nM 2′-dG (in a 1:1 binding model). Importantly, this riboswitch could bind 2′-dG at approximately two orders of magnitude stronger than guanosine (only differed by a 2′-OH). One of the explanations was that the mutated regions were located in the upstream of genes encoding ribonucleotide reductase subunits, which converted ribonucleotides into the deoxyribonucleotide counterparts. Therefore, the engineered mRNA tended to exhibit a much higher affinity for 2′-dG than dG.

Serganov et al. solved the crystal structure of this 2′-dG riboswitch [68]. They found its binding pocket was very different from that of the guanine riboswitch. The mutation led to rearrangements of the RNA, resulting in accommodation of an additional sugar moiety, and the 2′-dG was able to fit in, but guanosine (with an extra -OH on the 2′ position) can just weakly bind. The binding affinity of guanosine decreased by a factor of 100 as reported by the original paper [67] and reduced by 50 using isothermal titration calorimetry (ITC) in this work.

3.3. Riboswitch for c-di-GMP

Bis-(3′–5′)-cyclic dimeric guanosine monophosphate (c-di-GMP) is a ubiquitous second messenger in bacteria, regulating biological processes ranging from biofilm formation to expression of virulence genes [69]. A class of riboswitches named GEMM was found to bind c-di-GMP for regulating gene expression. Among them, the Vc2 RNA had a K_d of ~1 nM c-di-GMP, which was recognized as the tightest RNA-small molecule interactions. It was about 1000 times tighter than the c-di-GMP binding protein (called *Escherichia coli* PilZ) [70]. The structures of the Vc2 riboswitch was solved by the Strobel group (at 2.7 Å resolution) [66, 71], and the Amaré group (at 3.2 Å resolution) [69]. The structure reported by Strobel et al. is shown in Fig. 5C, in which the c-di-GMP was specifically and asymmetrically recognized by two highly conserved nucleotides G_{20} and C_{92} [66].

This riboswitch for c-di-GMP was developed to a few fluorescent biosensors due to its structure adaptability in different systems. The binding of c-di-GMP was transduced by introducing fluorescent 3,5-difluoro-4-hydroxybenzylidene imidazolinone (DFHBI) [72, 73]. Since the c-di-GMP folded RNA shared a critical stem for binding DFHBI, such binding increased the fluorescence. Hammond and coworkers covalently modified DFHBI into the riboswitch, and used this platform to sense both the extracellular [73] and intracellular c-di-GMP [72]. About 30-fold fluorescence elevation was observed for c-di-GMP, while none of the analogues including cGMP, rGMP, GMP and other nucleotides showed a signal change. Through introducing the DFHBI, the apparent K_d was measured to be 230 ± 50 nM c-di-GMP, and 1 μM c-di-GMP was detectable.

3.4. Riboswitch for inosine monophosphate

While riboswitches are naturally found, they can also be artificially created by fusing an existing RNA aptamer (as a target binding domain) with a conformational change domain in existing riboswitches. For example, Sugimoto et al. incorporated the in vitro selected xanthine aptamer in a thiamine pyrophosphate riboswitch, so that inosine monophosphate (IMP), a xanthine analogue, was able to bind tightly (K_d ~38 nM) [74]. Compared with the SELEX-derived aptamer, riboswitches are relatively larger (around 100-mer). Therefore, they are more difficult to be developed into biosensors, especially for applications outside cells [65].

4. Rationally designed DNA sequences

Compared to the vast amount of work on DNA aptamers for adenine derivatives [75], DNA aptamers for guanine derivatives were rarely reported. Recently, several non-SELEX-derived DNA sequences for recognizing guanine derivatives have been reported, and some took advantage of G-quadruplex structures [76].

4.1. Deleting a guanine nucleobase

In 2003, the Teramae group proposed that when removing a nucleobase from a DNA duplex, the resulted abasic site was able to rebind the deleted base through base pairing or pseudo base pairing [22, 23]. An abasic site can be obtained by introducing a tetrahydrofuranyl residue (dSpacer) lacking a nucleobase moiety or a propylene residue (Spacer

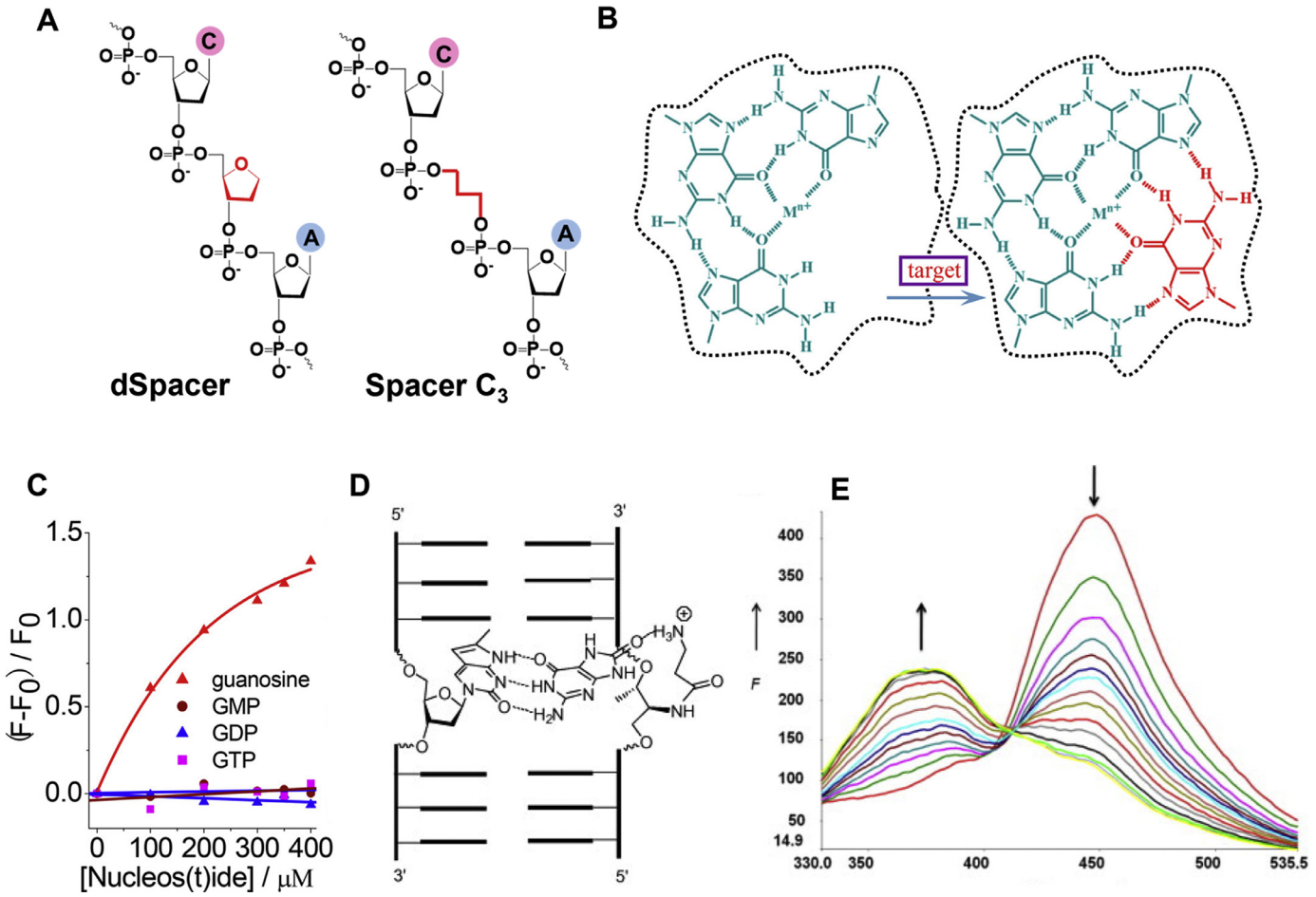

Fig. 6. (A) Structures of abasic sites named dSpacer and Spacer C3. (B) Free guanosine fits into an abasic site-containing G-quadruplex. (C) ThT binding assays for guanosine, GMP, GDP and GTP to an abasic site-containing G-quadruplex. Reproduced with permission [77]. Copyright 2018, American Chemical Society. (D) Chemical interactions between 8-oxoG and pyrrolo-dC in an abasic site-containing DNA duplex. (E) Fluorescence titration of an abasic site-containing duplex with 8-oxoG. Reproduced with permission [80]. Copyright 2012, Elsevier Ltd.

C_3) as shown in Fig. 6A. Inspired by these findings, Yin et al. recently removed a guanine in a G-quadruplex scaffold (Fig. 6B). Based on the formation of a full G-quartet in the presence of K^+, guanosine was able to fit into the vacancy [77]. This recognition was studied by using thioflavin T (ThT) as a label-free fluorescent probe, with a detection limit of 5 μM guanosine. Fig. 6C shows that the larger GMP, GDP and GTP cannot bind. Therefore, a single phosphate difference between guanosine and GMP was distinguished in this case.

Galeone et al. pointed out that the insertion of a dSpacer as an abasic site can significantly destabilize G-quadruplex, while introducing a dSpacer near the 3′ terminus is even worse than that near the 5′ terminus [78]. Therefore, care needs to be taken for designing abasic site-contained G-quadruplexes. Recently, through introducing a hairpin structure in an abasic site-contained G-quadruplex, Chen and coworkers improved the detection limit for guanine down to 18.3 nM (also probed by ThT) [79].

In addition to G-quadruplex scaffolds, abasic site-containing DNA duplexes were also investigated. Huang et al. modified the opposite strand of an abasic site by fluorescent pyrrolo-dC (pC) to specifically sense 8-oxo-7,8-dihydroguanine (8-oxoG) [80], a major product of guanine oxidation during DNA damage (Fig. 6D) [81]. Adding 8-oxoG quenched about 70% of the pC fluorescence at 446 nm, whereas the fluorescence at 380 nm increased (Fig. 6E). The K_d of binding 8-oxoG was measured to be 5.5 ± 0.8 μM, with a detection limit of 100 nM. Guanine (K_d ~15 μM) bound around 3-times weaker than 8-oxoG, and other nucleobases showed K_d from 22 to 34 μM.

4.2. *Deleting an entire guanine nucleotide*

Since introducing abasic site-contained DNA needs special synthetic steps, using unmodified DNA would be more attractive. The Tan group spliced an entire guanine nucleotide instead of guanine nucleobase from a G-quadruplex [24]. This way, only an unmodified DNA was synthesized, but a vacancy in its secondary structure may form (left panel of Fig. 7A). They found that when this vacancy appeared in top layer of the G-quadruplex, it was able to bind a few guanine derivatives, such as guanosine, GMP, GDP and GTP (right panel of Fig. 7A). Since negatively charged phosphate groups tend to be repelled by DNA backbone, the affinities to GMP, GDP and GTP gradually decreased. Other nucleosides and nucleotides cannot bind at all. These binding reactions were evaluated by DMS footprinting and DNA melting experiments. The footprinting data in Fig. 7B shows that guanosine binding was only achieved in the presence of K^+, indicating the formation of a G-quartet.

Later, they further developed this system into a fluorescent sensor by extending this vacancy-bearing G-quadruplex strand with a hybridized domain, and then respectively label the two ends with a fluorophore and a quencher (the left panel in Fig. 7C). The fluorescence was quenched in the initial stage. After adding guanosine or GMP, under the driving force of forming the G-quadruplex, the loop part switched the structure leading to increased fluorescence (Fig. 7C) [82]. However, apart from GMP, other analytes like xanthosine, 8-oxo-2′-deoxyguanine (a biomarker of DNA damage), and two more guanine-related drugs (Ganciclovir and Acyclovir) all increased the fluorescence signal.

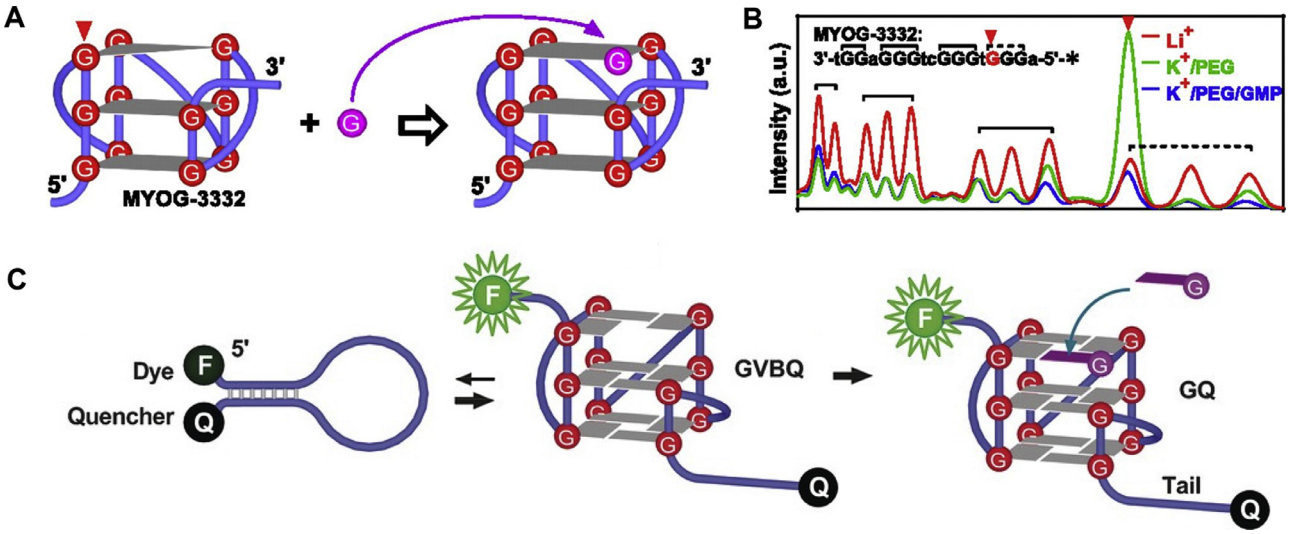

Fig. 7. (A) Schematic illustration of free guanine-containing ligands fitting into the vacancy in the top layer of the G-quadruplex. (B) Quantification of DMS footprinting results for a vacancy-bearing G-quadruplex upon binding guanine-containing ligands. Reproduced with permission [24]. Copyright 2015, National Academy of Sciences. (C) Schematic illustration of a defective G-quadruplex based fluorescent sensor for specific binding guanine-containing compounds. Reproduced with permission [82]. Copyright 2016, Wiely-VCH.

Yang and coworkers investigated a vacancy-bearing G-quadruplex sequence from a human gene promoter named PDGFR-β [83]. They measured various K_d values for guanine derivatives on microscale thermophoresis (MST) from 3.1 ± 0.4 μM (for deoxyguanosine) to 511 ± 44 μM (for dGTP). Using NMR, they found that the binding of dGTP involved Hoogsteen hydrogen bonding, coordination with K^+ and base stacking. An additional C1′-H1′•••O4′ (a nonconventional CH•••O hydrogen bond) may also exist.

4.3. Guanine-excised aptamers

Aside from engineering G-quadruplexes, our group recently proposed a cost-effective and highly specific strategy to recognize guanosine based on base excision, in which an aptamer was used as a scaffold and an entire guanine nucleotide was removed to generate a breaking point. This is different from the above splicing strategy since the strand was broken after the excision, and a new 3′ and a new 5′ were generated. As described in Fig. 8A, the excised site can act as a binding pocket to specifically accommodate the deleted purine nucleoside [25].

We used both the adenosine aptamer (Fig. 8B) and the Na^+-binding aptamer embedded in a Ce13d DNAzyme [84–86] (Fig. 8C) as scaffolds for detecting guanosine [26]. The four guanines in adenosine aptamer (G_8, G_9, G_{18} and G_{19}) and three guanines in Na^+ aptamer (G_{14}, G_{15} and G_{16}) were individually excised. Based on SYBR Green I (SGI) and ThT fluorescence spectroscopy, we found that the G_{16}-excised adenosine aptamer (Fig. 8D) and G_{19}-excised Na^+-aptamer (Fig. 8E) exhibited most notable specificity for free guanosine, but not for GMP. The apparent K_d for guanosine was measured to be 0.78 mM and 0.32 mM for the G_{16}-exicsed adenosine aptamer and G_{19}-excised Na^+-aptamer, respectively.

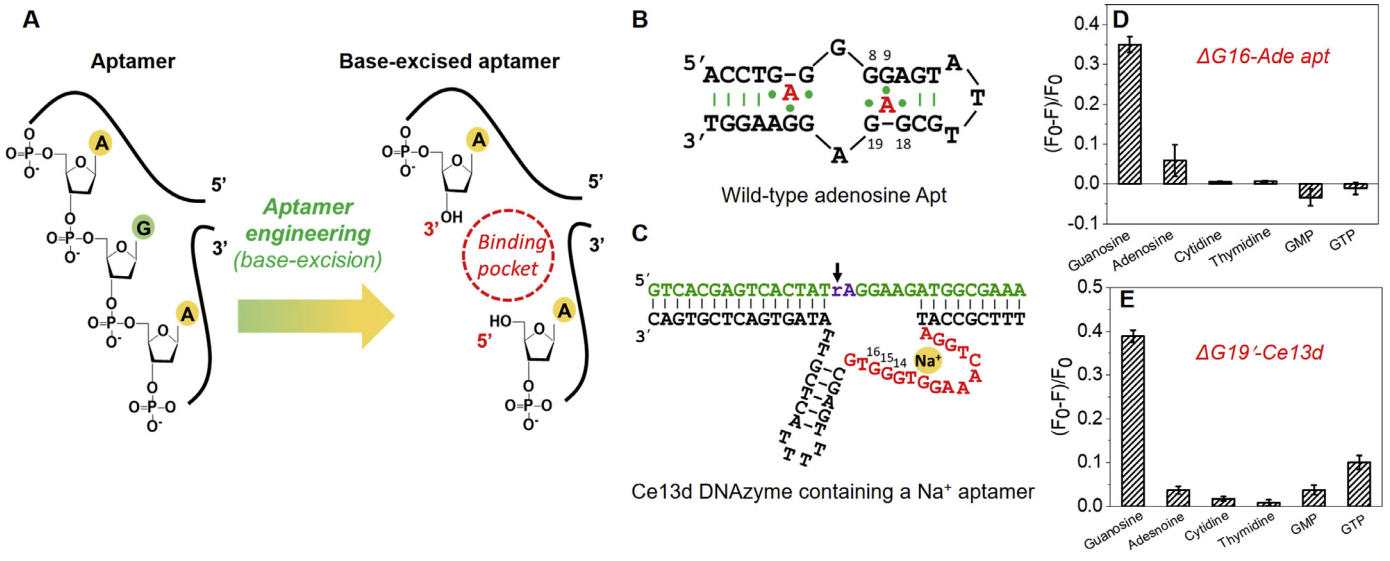

Fig. 8. (A) Scheme for base-excision strategy. An entire guanine nucleotide is removed from an aptamer scaffold, and a break is generated. The break is able to specifically re-bind free guanosine but cannot accommodate GMP. The secondary structure of the (B) wild-type adenosine aptamer, and (C) Ce13 DNAzyme. Selectivity for the (D) G_{16}-excised adenosine aptamer, and (E) G_{19}-excised Na^+-aptamer based on dye staining fluorescence spectroscopy. Reproduced with permission [26]. Copyright 2020, Wiley-VCH.

5. Protein based recognition

Since guanine is a nucleobase, using nucleic acids as ligands for their binding can harness base pairing and G-quadruplex interactions. Before the advent of aptamers, biosensors for molecular recognition mainly relied on proteins. For example, protein-based enzymes and antibodies are useful platforms. A few proteins are also able to specifically recognize guanine and its derivatives.

5.1. G-proteins for recognizing GTP

G-proteins belong to a large family of hydrolase enzymes that can bind GTP and hydrolyze it to GDP [87, 88]. Unger et al. found a polytopic membrane protein FeoB (a typical G-protein) with a guanine nucleotide binding domain exhibiting a K_d of 4–15 μM for GTP (Fig. 9A) [89]. Nikiforov recently pointed out that a tight binding for GTP might not always be desirable, especially when measuring it in cells, because the total cellular GTP is 300–800 μM [90]. A too strong affinity may saturate sensor signals.

To solve this problem, Nikiforov et al. inserted a circularly permuted yellow fluorescent protein (cpYFP) into this FeoB to obtain an engineered G-protein for sensing intracellular GTP [90]. In the residues 35–40 of the FeoB G-protein region, the cpYFP was introduced (Fig. 9B). They measured K_{eff} values (the GTP concentrations required to obtain 50% of the maximal ratiometric signal) of five engineered proteins to be from 30 to 2000 μM, sufficient to cover the intracellular GTP concentrations. Among these proteins, one candidate named FY5a + 5a showed a ratiometric fluorescence change upon adding GTP (e.g. an emission decrease with 405 nm excitation and an emission increase with 485 nm excitation). Therefore, a larger change was obtained by using the ratio of their emission intensities (Ex405/Ex485). Both GTP and dGTP (4 μM) induced about a 40% signal change in this ratio, whereas 500 μM CTP, UTP, ATP and ITP had little

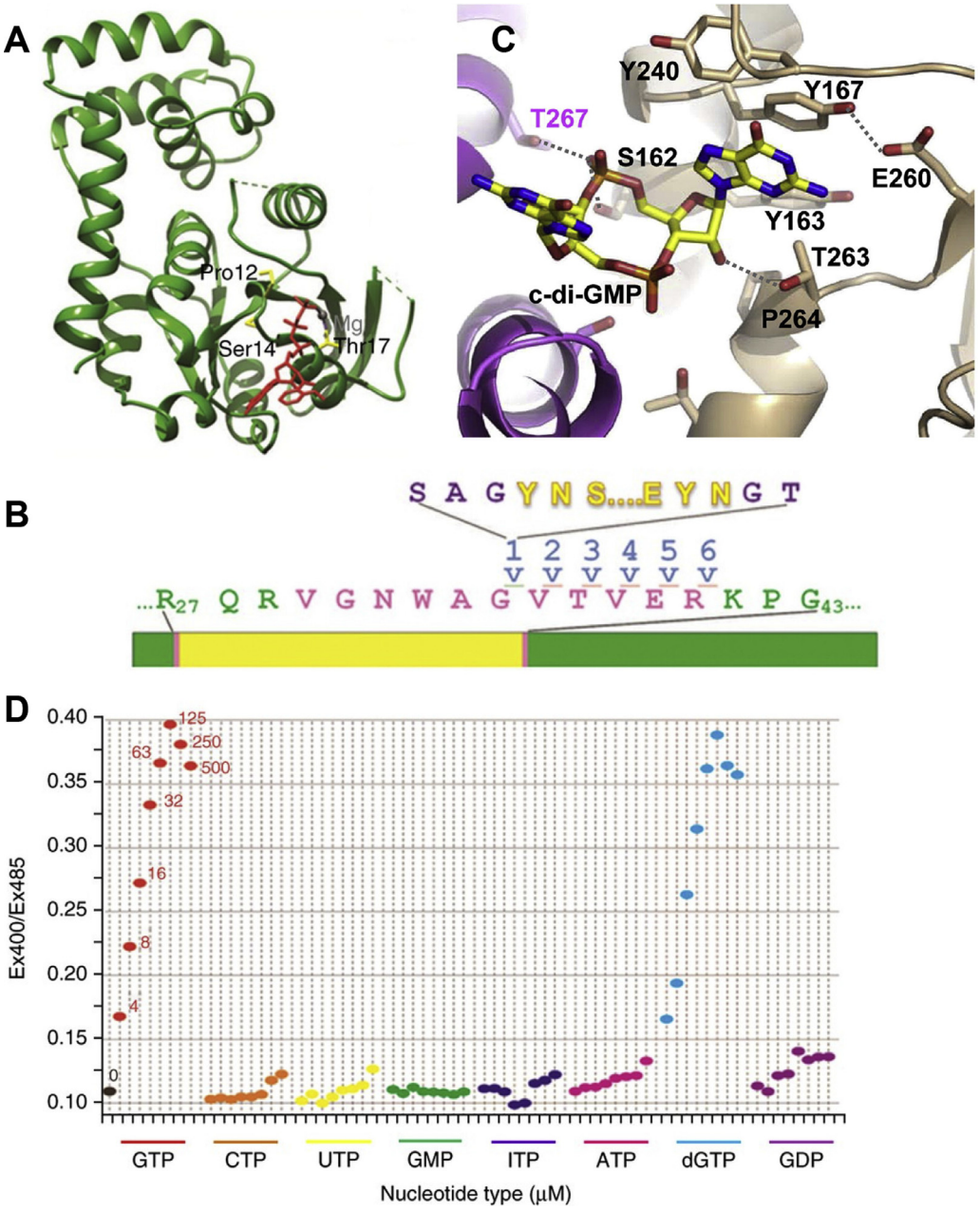

Fig. 9. (A) The G-protein domain of the FeoB protein binding with a GTP. (B) The DNA encoding cpYFP was inserted into that for the FeoB G protein corresponding to the residues 35–40. (C) The detailed interaction between c-di-GMP and STING. Reproduced with permission [91]. Copyright 2012, Elsevier Inc. (D) Specificity of the engineered cpYFP. Reproduced with permission [90]. Copyright 2017, Nature America, Inc.

effect (Fig. 9D). Since the dGTP level in proliferating cells is 100-fold lower than GTP, interference from dGTP became negligible. Importantly, GMP and GDP also showed < 10% response in Fig. 9D, indicating a very high specificity of this sensor in live cells. From this example, the specificity of a sensor not only relies on the binding ligand, but also greatly affected by its actual detection environment. The specificity in test tubes may not be equal to that in live cells.

5.2. STING for c-di-GMP

A transmembrane protein called STING (stimulator of interferon gene) that can specifically bind c-di-GMP was found by Vance et al. in 2011 [92]. The STING acts as an innate immune sensor for this cyclic dinucleotide to simulate the activity of type I interferons (IFNs). The K_d of STING binding to c-di-GMP was measured at about 5 μM by equilibrium dialysis [92].

Inspired by this finding, Wu and coworkers studied the structural features of the c-di-GMP binding domain of STING by X-ray crystallography [91]. They used the difference map to demonstrate that a c-di-GMP was able to bind to the central crevice of a STING dimer through stacking and hydrogen bonding. The detailed interaction is shown in Fig. 9C, in which most interactions to c-di-GMP were provided by Y167, and other residues including E260 contributed to multiple van der Waals and hydrogen bonding interactions. Since the STING also can bind c-di-AMP through Y167 but not E260, its affinity for c-di-AMP appeared lower. Other groups also carried out independent researches on STING to further understand its functions with c-di-GMP [93–95]. c-di-AMP but not GTP or ATP can also bind STING (with lower affinities, K_d not determined) [92]. Using STING for detecting c-di-GMP has yet to be demonstrated.

6. Small molecule-based sensors

Apart from the large amount of works using biological recognition molecules such as nucleic acids and proteins to achieve guanine detection, studies were also carried out using small molecule based chemosensors.

6.1. Imidazolium for sensing GTP

Imidazole is a heterocyclic aromatic molecule, and it appears in the side chain of histidine. In sensing applications, its salt imidazolium was developed for detecting purine nucleotides. A series of imidazolium-based cyclophanes were synthesized for detecting GTP [27–30]. For example, Kim et al. designed a compound shown in Fig. 10A, synthesized by the reaction of 1,8-bis-(bromomethyl)anthracene with 1-(1*H*-imidazol-1-ylmethyl)−1*H*-imidazole in anhydrous DMF [29]. This compound had blue fluorescence emission. Binding of GTP induced a unique green fluorescence (Fig. 10B). GTP quenched the blue fluorescence peaks and red-shifted the peak to 490 nm by forming a GTP-cyclophane excimer (Fig. 10C). The guanine base in GTP acted as the quencher in this case. Other nucleotides cannot bind to cyclophane, thereby failed to change its emission wavelength. The K_d for GTP was determined to be 1 μM, and the interaction between GTP and cyclophane was characterized through formation of a $(C—H)^+ \bullet\bullet\bullet anion^-$ hydrogen bond. The limit of detection was determined to be 0.97 μM.

Wang and Chang synthesized two benzimidazolium dyes. As shown in Fig. 10D, the X position can be either a hydrogen or a fluorine [27]. The two structurally related compounds both showed dramatically increased fluorescence upon adding GTP. Particularly, when the X = H, 80-fold fluorescence increase at 540 nm was observed upon adding GTP, whereas the changes by adding other nucleotides such as ATP were close to zero (Fig. 10E). The fluorescence increase was also visible in a 96-well plate (inset of Fig. 10E). They speculated that both the imidazolium and 2-phenylindole moiety in the dye were important for specific GTP recognition. The K_d for binding GTP (when X = H) was measured to be 33 μM, although the LOD was not reported.

6.2. Thiazole orange for sensing c-di-GMP

Thiazoles have a similar structure to imidazole, and thiozole orange (TO) is a well-known fluorescent intercalator for polynucleotides. The intercalation and minor groove binding can lead to its restricted rotation and thereby fluorescence enhancement. Typically, TO is non-fluorescent

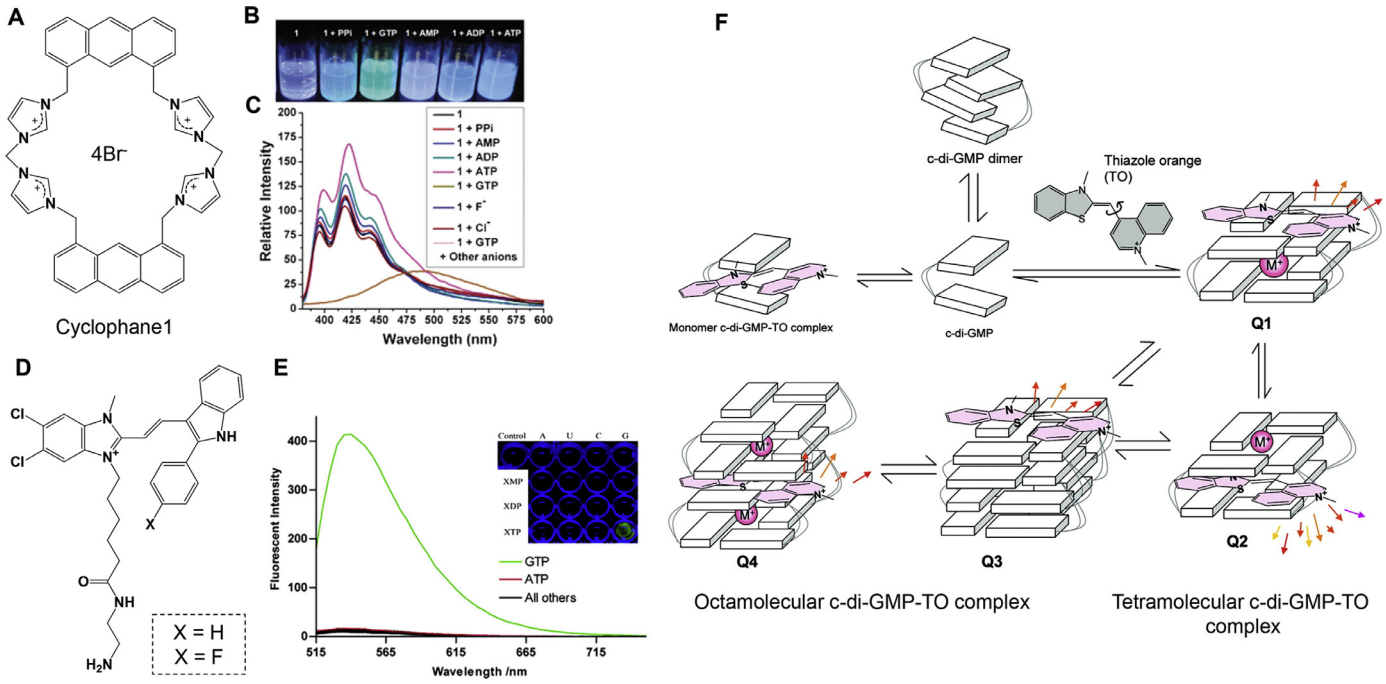

Fig. 10. (A) The chemical structure of cyclophane 1. (B) Visual fluorescence features, and (C) fluorescence spectrum showing the binding specificity of the cyclophane 1 to GTP. All reproduced with permission [29]. Copyright 2012, Royal Society of Chemistry. (D) The chemical structure of benzimidazolium dye. (E) Binding specificity of the benzimidazolium dye to GTP. All reproduced with permission [27]. Copyright 2006, American Chemical Society. (F) The scheme of TO forms tetramolecular quadruplex (Q1 and Q2) and octamolecular complex (Q3 and Q4) with c-di-GMP. Reproduced with permission [96]. Copyright 2011, American Chemical Society.

when incubated with free nucleotides, such as guanosine and GTP. However, Sintim et al. found an exception that it can be a specific probe for a dinucleotide c-di-GMP, because c-di-GMP can self-aggregate forming a G-quartets in the presence of K^+ (Fig. 10F) [96, 97]. The authors hypothesized that the c-di-GMP can form 4:1 complex with TO (Q1 and Q2 in Fig. 10F), or 8:1 complex (Q3 and Q4). TO binding was confirmed by the red shift in its absorption spectrum and circular dichroism (CD). None of the other nucleotides including GTP, cGMP, and c-di-AMP induced any fluorescence signal. The detection limit for this assay was 5 μM.

7. Electrochemical sensors

The above methods for recognizing guanine and its derivatives mostly used fluorescence for signaling, and recognition was based on molecular interactions. In electrochemical sensors, the mechanism of electro-oxidation of guanine is shown in Fig. 11A, in which guanine was converted to 8-oxoguanine. The oxidation potential for guanine is the lowest among the four nucleobases, followed by adenine (just slightly higher), thymine and cytosine [98]. For example, on an Ag/AgCl electrode, free guanine is oxidized at +0.7 V, adenine at +0.97 V, thymine at +1.15 V, and cytosine at +1.13 V (at pH 7) [99]. For the electrochemical sensors described in this section, the redox peaks were used for identification of guanine and no affinity molecules were required. Given that the slow electron transfer kinetics of nucleobase, sensing guanine on bare electrode often faces problems of low sensitivity [100, 101]. Therefore, materials, such as carbon nanotubes, graphene, precious and transition metals and polymers, are generally used to modify electrodes to modulate the electrochemical oxidation.

7.1. Carbon-modified electrodes

When carbon atoms are packed in a single layer of sheets or tubes, they form graphene and carbon nanotubes respectively with excellent electrical conductivity and a large specific surface area [102]. Efforts have been made to develop graphene and carbon nanotube containing electrical devices. Xiong et al. used -COOH functionalized graphene to modify a glassy carbon electrode (GCE), and realized simultaneous determination of guanine and adenine. The -COOH groups made the graphene more hydrophilic and easier to be dispersed. Since the redox potential of guanine is only slightly lower than adenine, guanine cannot be differentiated with adenine [103]. The detection limit of guanine in this case was 50 nM.

7.2. Metals and metal oxides-modified electrodes

Metals and metal oxides, such as doped Au, Ag, Pt, Pd, Cu and iron oxide and zinc oxide, were also used to modify the electrode due to their

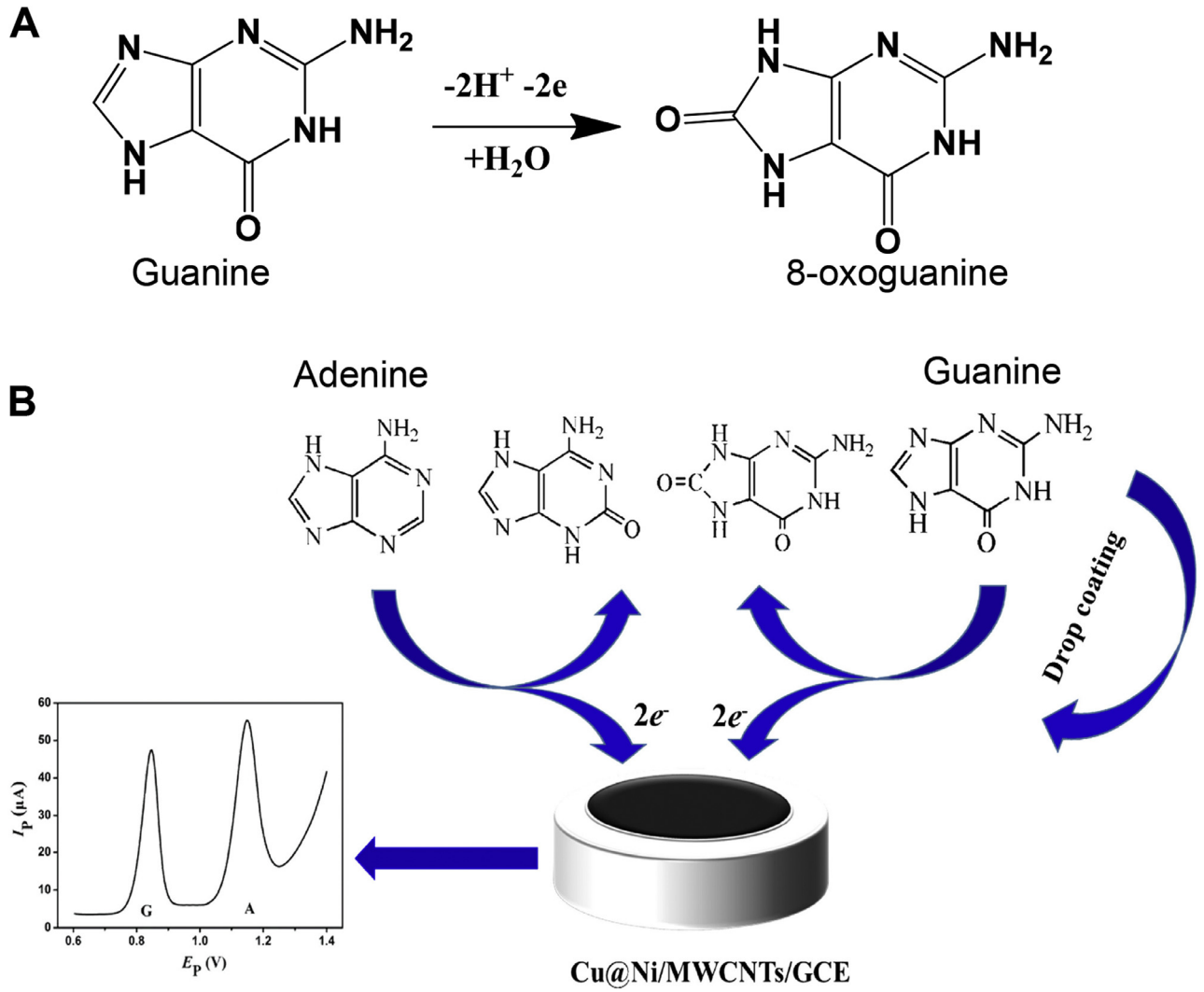

Fig. 11. (A) The oxidation of guanine to 8-oxoguanine. (B) The scheme of Cu@Ni/MWCNTs sensing system for guanine and adenine. Reproduced with permission [104]. Copyright 2018, Elsevier B.V.

good electrical conductivity and catalytic activity. For example, Li et al. doped copper and nickel ($NiCl_2$ and $CuSO_4$ as sources) to multi-walled carbon nanotubes (Cu@Ni/MWCNTs) [104]. By using this bimetallic catalyst, the catalytic ability improved due to the unique 3d band holes of Ni and superior electron transfer capacity from the single electron of 4 s band of Cu. Under positive potentials, both guanine and adenine were oxidized (Fig. 11B). Their simultaneous detection was realized, but not for thymine and cytosine. The detection limits for G and A were at 0.17 μM and 0.33 μM, respectively. Such simultaneous sensing has been reported by many independent groups, although specific oxidation of guanine was less mentioned because of its oxidation potential being just slightly lower than that of adenine.

Santhanalakshmi et al. prepared oleylamine-capped CuO nanoparticles on MWCNTs, and achieved the sensing of guanosine with a LOD of 0.084 μM [105]. Due to the similar operating potential of guanosine and adenosine, adenosine cannot be distinguished. Recently, Lu and coworkers reported a Ni-Fe Prussian blue analog hollow nanocube (Ni-Fe PBA HNCs) to specifically detect guanine, and it was unresponsive to adenine [106]. The PBA was composed of multiple metal ions and cyanogen, and the redox of the multiple metal ions in the PBA can provide a channel for electrons. Since the PBAs can lower the potential for electrocatalysis, the oxidation of guanine became easier. This way, the potential difference between guanine and adenine was widened, and then the specific oxidation of guanine can be realized, leaving adenine intact. The detection limits for guanine was measured at 10.4 nM.

7.3. Polymer-modified electrodes

In addition to metal and metal oxides, conducting polymers are another modifiers to facilitate the oxidation of guanine because of their inherent charge transport properties and excellent redox responses [107, 108]. Among the conducting polymers, organic dyes-based polymers have gained the most interest because of their high conductivity and facile preparation process on electrode (through electropolymerization) [108–110]. Taking a thionine dye as an example [109], Fang et al. adsorbed polythionine on a carbon electrode (through π-π stacking) to sense guanine and adenine [111]. Such adsorption improved the electron transfer from polymer surface to electrode. The detection limits of such sensor for guanine and adenine were 10 nM and 8 nM, respectively. Apart from thionine, other dyes like poly(methylene blue) [112] and poly(alizarin red) [113] were also reported.

In addition to organic dyes, overoxidized polymers were also used for guanine detection. Due to overoxidization, such polymers were found to have a low background current and good sensitivity. For example, Wu and coworkers modified overoxidized polypyrrole (PPy) on a graphene-coated electrode for the detection of guanine and adenine [114]. The oxygen containing groups such as carbonyl and carboxyl were introduced to pyrrole unit during the overoxidation process, resulting in improved electron transfer efficiency. The detection limits of guanine and adenine were 10 nM and 20 nM in this case, respectively. Similarly, overoxidized polyimidazole was also used by Lu and coworkers for sensing purines [115].

8. Nanomaterial based sensors

Some nanomaterials were also used for guanine recognition. The first example is the quantum dot (QD)-based ratiometric fluorescence probe reported by Hu et al. In this work, intrinsic dual-emitting ZnCdTe QDs were synthesized by using fluorescence S-doped-carbon dots (CDs) as capping ligands, named as CDs-ZnCdTe QDs (left panel of Fig. 12A). This composite has one emission peak at 420 nm from the CDs and the other at 605 nm from the QDs [116]. The fluorescence emission of the

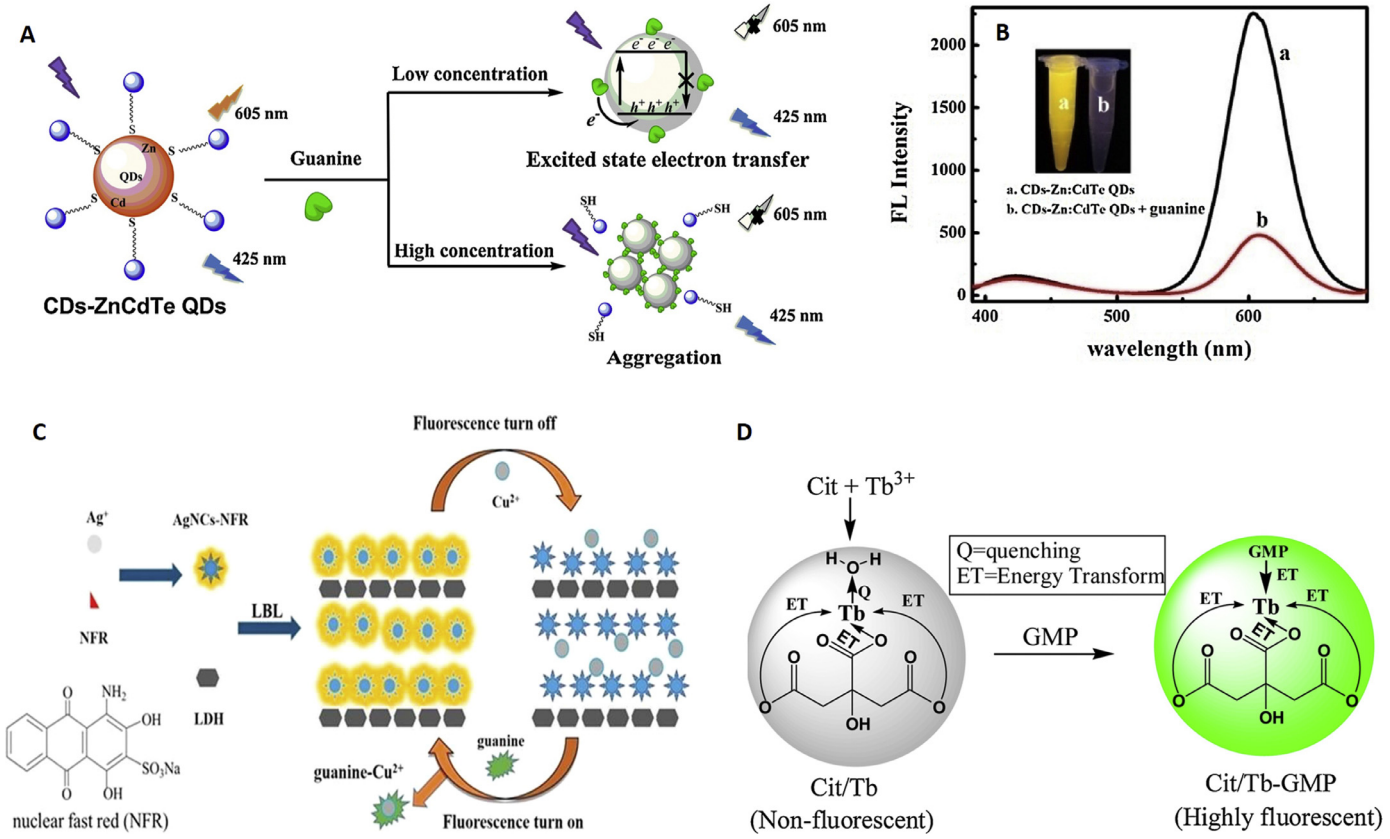

Fig. 12. (A) Scheme of a ratiometric sensing system based on CDs-ZnCdTe QDs. (B) Fluorescence spectra of adding guanine into the CDs-ZnCdTe QDs. All reproduced with permission [116]. Copyright 2018, Elsevier B.V. (C) The scheme of AgNCs-NFR/LDH-Cu^{2+} sensing system. Reproduced with permission [117]. Copyright 2018, Elsevier B.V. (D) The scheme of Cit/Tb sensing system. Reproduced with permission [120]. Copyright 2019, Elsevier B.V.

CDs was stable, while that of QDs was quenched by guanine. Low concentration of guanine quenched the fluorescence via excited state electron transfer, while high concentration of it can release the S-doped CDs from the CDs-ZnCdTe QDs and then resulted in the aggregation of QDs. Based on these two mechanisms, ratiometric sensing (I_{605}/I_{425}) of guanine was realized (Fig. 12A). As shown in Fig. 12B, over 5-fold fluorescence decrease in the 605 nm peak was observed, while the 425 nm peak remained constant. None of the other purines including adenine and xanthine quenched the fluorescence. The detection limit of guanine was determined to be 0.076 μM. However, the guanine derivatives were not tested. In addition, it cannot rule out that other quenchers might also produce a similar fluorescence quenching.

Jin et al. designed a fluorescent silver nanocluster (AgNC)-based sensor immobilized on layered double hydroxides (LDHs) [117]. To endow this platform with fluorescence sensing functionality, a nuclear fast red (NFR) dye was used and interacted with the AgNCs in the initial status (Fig. 12C). The AgNCs-NFR complex had strong fluorescence. However, when adding Cu^{2+} into the system, the fluorescence was quenched due to the formation of NFR-Cu^{2+} conjugates. Since the guanine had stronger coordination with Cu^{2+} than NFR, further adding guanine recovered the fluorescence. Guanine increased the fluorescence intensity by about 3-fold, whereas the signal of adenine was half of the guanine, and the signals from the pyrimidines were even less. The detection limit of guanine was 1.85 μM. It is likely that other chelators for Cu^{2+} might also produce a signal recovery, such as glutathione (GSH) [118] and GMP [119].

To determine GMP, Xu and coworkers created lanthanide coordination polymer nanoparticles (LCPNPs) composed of terbium ions (Tb^{3+}) and citrate (Cit) [120]. The Cit/Tb^{3+} alone did not have luminescence in water, because water can coordinate to Tb^{3+}, enabling the energy transfer to water. Since GMP can strongly coordinate with Tb^{3+}, the water molecules were replaced. In addition, due to the energy transferred from GMP to the emissive $^5D_4$ state of Tb^{3+} (Fig. 12D), about 15-fold fluorescence increase was achieved. AMP, CMP, UMP or IMP did not trigger any obvious fluorescence enhancement due to their low affinity and mismatched energy with Tb^{3+}. The detection limit for GMP was 100 nM. Compared to the two previous examples, this was a light-up sensor.

9. Molecularly imprinted polymer-based sensors

The final mechanism of target recognition discussed here relies on molecularly imprinted polymers (MIPs). MIPs are praised as "artificial antibody" that can work like natural antibody to accept shape complementary and chemical complementary ligands, but are much more stable and robust, as they are synthetic polymers. Hartell et al. reported a fluorescent MIP for guanosine 3′,5′-cyclic monophosphate (cGMP) [121]. They used 2-acrylamidopyridine as the fluorescent monomer, trimethylolpropane triacrylate (TMPTA) as the crosslinker, and 2,2′-azobis(2-methylpropionitrile) as the initiator to imprint cGMP through free radical polymerization. After reaction, the cGMP was removed by methanol/water mixture (3:7, v/v). Based on their fluorescence data, the MIP was able to re-bind cGMP with about 2.5-fold decreased signal, whereas analogs like GMP and cAMP did not make any difference, although the detection limit was not reported.

10. Conclusion and future perspective

In summary, we have reviewed various strategies to recognize guanine and its derivatives, ranging from nucleic acids, proteins, small organic molecules, MIPs to nanomaterials. The signaling strategies largely rely on fluorescence and electrochemistry. Most guanine-related aptamers are RNA, making their detection much less explored due to the unstable nature of the RNA molecules. Comparatively, for adenine, a number of high-quality and robust DNA aptamers are available. Therefore, the detection of adenine derivatives has been much more performed. In general, nucleic acid and protein-based recognition of guanine derivatives has the highest specificity, especially the riboswitches. The guanine riboswitch exhibits 100,000-fold higher binding affinity than adenine, and the tightest RNA-small molecule interaction (K_d ~1 nM) is from the c-di-GMP riboswitch. However, the size of the aptamers in riboswitches is much larger compared to SELEX-derived aptamers. Due to their large size and the low stability, using riboswitches as biosensors for detection outside cells is less appealing [65].

Although the number of guanine related DNA aptamers from SELEX is limited, some non-SELEX-derived aptamers have been reported. Abasic site-containing G-quadruplex and duplex, vacancy-bearing G-quadruplex, and base-excised aptamers were exploited. Apart from the nucleic acid-based molecular recognition, proteins also exhibit specific and tight binding for guanine derivatives. This recognition largely relied on their shape complementary and chemical complementary to the ligands. MIPs, which aimed to mimic biological molecular recognition, were also developed to specifically bind guanine-related compounds. In addition, due to the specific interactions with guanine base, several small organic molecules and nanomaterials were also exploited, although their recognition may not be as selective as aptamers, proteins and MIPs.

From the signal transduction point of view, fluorescent sensors were used more widely than electrochemical sensors, likely due to the simpler sample preparation and low background of homogeneous fluorescent assays. Electrochemical sensors are advantageous for in situ measurement and in vivo studies since fluorescence probes are limited by the short tissue penetration depth and background fluorescence. Electrochemical sensors have mainly relied on the intrinsic redox properties of guanine, making the specificity low, especially interference from adenine. Attaching affinity ligands such as aptamers and MIPs might be used to improve specificity.

In future studies, we believe more selections can be performed to obtain new DNA aptamers for guanine-related ligands. High-quality DNA aptamers are more likely to be further applied in various analytical applications. Given that excellent riboswitches for guanine exist and DNA aptamers for adenine also exist, it should be chemically feasible to obtain DNA aptamers for guanine derivatives. To improve the binding specificity of the DNA aptamer, both the library and elution protocols need to be prudently designed. We have not seen a lot of MIP-based guanine sensing work, and by introducing DNA into MIPs, both guanine binding and sensing might be improved [122, 123]. Since the guanine and guanosine have low water-solubility, an oil phase like toluene and acetonitrile are good choice to imprint for them. In contrast, for hydrophilic guanine nucleotides, water-based buffers are preferred. Considering that the free radical polymerization-derived polymers tend to have uncontrolled pore size and heterogeneous binding performances, advanced fragmentation chain transfer polymerization (RAFT) might be able to generate well-controlled and finely structured binding pockets.

In addition, although protein-based strategies can also highly specifically recognize a few guanine derivatives, the stability and cost problems of the proteins have limited their broader applications. Some artificial protein mimic such as nanozymes [124–126] can be designed to mimic the function of proteins with improved robustness and lower cost. Finally, impactful applications in biology and biomedical diagnosis need to be demonstrated to further stimulate the fundamental sensing work. By performing practical sensing studies, we can learn critical technical barriers and sample matrix effect, which would in turn guide sensor development.

Declaration of Competing Interest

There are no conflicts to declare.

Acknowledgements

We thank M. Kushalkar for proofreading this manuscript. Funding for the Liu lab portion of the work reviewed here was mainly from The

Natural Sciences and Engineering Research Council of Canada (NSERC) Grant STPGP 447472-13.

References

[1] A.P. Schmidt, D.R. Lara, J. de Faria Maraschin, A. da Silveira Perla, D. Onofre Souza, Guanosine and GMP prevent seizures induced by quinolinic acid in mice, Brain Res. 864 (2000) 40–43.

[2] C.I. Tasca, D. Lanznaster, K.A. Oliveira, V. Fernández-Dueñas, F. Ciruela, Neuromodulatory effects of guanine-based purines in health and disease, Front. Cell. Neurosci. 12 (2018) 376.

[3] C.A. Droppelmann, D. Campos-Melo, K. Volkening, M.J. Strong, The emerging role of guanine nucleotide exchange factors in ALS and other neurodegenerative diseases, Front. Cell. Neurosci. 8 (2014) 282.

[4] M.Z. Gilcrease, S.K. Kilpatrick, W.A. Woodward, X. Zhou, M.M. Nicolas, L.J. Corley, et al., Coexpression of $\alpha 6\beta 4$ integrin and guanine nucleotide exchange factor Net1 identifies node-positive breast cancer patients at high risk for distant metastasis, Cancer Epidemiol. 18 (2009) 80–86.

[5] I.J. Oliveira, S. Molz, D.O. Souza, C.I. Tasca, Neuroprotective effect of GMP in hippocampal slices submitted to an in vitro model of ischemia, Cell. Mol. Neurobiol. 22 (2002) 335–344.

[6] J. Yang, G. Xu, H. Kong, Y. Zheng, T. Pang, Q. Yang, Artificial neural network classification based on high-performance liquid chromatography of urinary and serum nucleosides for the clinical diagnosis of cancer, J. Chromatogr. B 780 (2002) 27–33.

[7] T. Paz-Elizur, R. Ben-Yosef, D. Elinger, A. Vexler, M. Krupsky, A. Berrebi, et al., Reduced repair of the oxidative 8-oxoguanine DNA damage and risk of head and neck cancer, Cancer Res. 66 (2006) 11683–11689.

[8] H.J. Helbock, K.B. Beckman, M.K. Shigenaga, P.B. Walter, A.A. Woodall, H.C. Yeo, et al., DNA oxidation matters: the HPLC–electrochemical detection assay of 8-oxo-deoxyguanosine and 8-oxo-guanine, Proc. Natl. Acad. Sci. U. S. A. 95 (1998) 288–293.

[9] F. Peyrane, B. Selisko, E. Decroly, J.-.J. Vasseur, D. Benarroch, B. Canard, et al., High-yield production of short GpppA-and 7MeGpppA-capped RNAs and HPLC-monitoring of methyl transfer reactions at the guanine-N7 and adenosine-2′ O positions, Nucl. Acids Res. 35 (2007) e26.

[10] K.-.Y. Wu, N. Scheller, A. Ranasinghe, T.-.Y. Yen, R. Sangaiah, R. Giese, et al., A gas chromatography/electron capture/negative chemical ionization high-resolution mass spectrometry method for analysis of endogenous and exogenous N 7-(2-hydroxyethyl) guanine in rodents and its potential for human biological monitoring, Chem. Res. Toxicol. 12 (1999) 722–729.

[11] A. Weimann, D. Belling, H.E. Poulsen, Quantification of 8-oxo-guanine and guanine as the nucleobase, nucleoside and deoxynucleoside forms in human urine by high-performance liquid chromatography-electrospray tandem mass spectrometry, Nucl. Acids Res. 30 (2002) e7.

[12] S.A. Yates, N.M. Dempster, M.F. Murphy, S.A. Moore, Quantitative analysis of malondialdehyde-guanine adducts in genomic DNA samples by liquid chromatography/tandem mass spectrometry, Rapid Commun. Mass Spectrom. 31 (2017) 762–770.

[13] S.D. Arnett, D.M. Osbourn, K.D. Moore, S.S. Vandaveer, C.E. Lunte, Determination of 8-oxoguanine and 8-hydroxy-2′-deoxyguanosine in the rat cerebral cortex using microdialysis sampling and capillary electrophoresis with electrochemical detection, J. Chromatogr. B 827 (2005) 16–25.

[14] R.R. Breaker, Prospects for riboswitch discovery and analysis, Mol. Cell 43 (2011) 867–879.

[15] A. Serganov, D.J. Patel, Metabolite recognition principles and molecular mechanisms underlying riboswitch function, Annu. Rev. Biophys. 41 (2012) 343–370.

[16] C. Tuerk, L. Gold, Systematic evolution of ligands by exponential enrichment: RNA ligands to bacteriophage T4 DNA polymerase, Science 249 (1990) 505–510.

[17] D.S. Wilson, J.W. Szostak, In vitro selection of functional nucleic acids, Annu. Rev. Biochem. 68 (1999) 611–647.

[18] K. Sefah, D. Shangguan, X. Xiong, M.B. O'Donoghue, W. Tan, Development of DNA aptamers using Cell-SELEX, Nat. Protoc. 5 (2010) 1169–1185.

[19] P.J.J. Huang, D. de Rochambeau, H.F. Sleiman, J. Liu, Target self-enhanced selectivity in metal-specific DNAzymes, Angew. Chem. Int. Ed. 59 (2020) 3573–3577.

[20] S.-.F. Torabi, P. Wu, C.E. McGhee, L. Chen, K. Hwang, N. Zheng, et al., In vitro selection of a sodium-specific DNAzyme and its application in intracellular sensing, Proc. Natl. Acad. Sci. U. S. A. 112 (2015) 5903–5908.

[21] D.E. Huizenga, J.W. Szostak, A DNA aptamer that binds adenosine and ATP, Biochemistry 34 (1995) 656–665.

[22] K. Yoshimoto, S. Nishizawa, M. Minagawa, N. Teramae, Use of abasic site-containing DNA strands for nucleobase recognition in water, J. Am. Chem. Soc. 125 (2003) 8982–8983.

[23] M. Li, Y. Sato, S. Nishizawa, T. Seino, K. Nakamura, N. Teramae, 2-Aminopurine-modified abasic-site-containing duplex DNA for highly selective detection of theophylline, J. Am. Chem. Soc. 131 (2009) 2448–2449.

[24] X.M. Li, K.W. Zheng, J.Y. Zhang, H.H. Liu, Y.D. He, B.F. Yuan, et al., Guanine-vacancy-bearing G-quadruplexes responsive to guanine derivatives, Proc. Natl. Acad. Sci. U. S. A. 112 (2015) 14581–14586.

[25] Y. Li, B. Liu, Z. Huang, J. Liu, Engineering base-excised aptamers for highly specific recognition of adenosine, Chem. Sci. 11 (2020) 2735–2743.

[26] Y. Li, J. Liu, Highly specific recognition of guanosine using engineered base excised aptamers, Chem. Eur. J. (2020), doi: 10.1002/chem.202001835.

[27] S. Wang, Y.-.T. Chang, Combinatorial synthesis of benzimidazolium dyes and its diversity directed application toward GTP-selective fluorescent chemosensors, J. Am. Chem. Soc. 128 (2006) 10380–10381.

[28] N. Ahmed, B. Shirinfar, I. Geronimo, K.S. Kim, Fluorescent imidazolium-based cyclophane for detection of guanosine-5′-triphosphate and I^- in aqueous solution of physiological pH, Org. Lett. 13 (2011) 5476–5479.

[29] N. Ahmed, B. Shirinfar, I.S. Youn, A. Bist, V. Suresh, K.S. Kim, A highly selective fluorescent chemosensor for guanosine-5′-triphosphate via excimer formation in aqueous solution of physiological pH, Chem. Comm. 48 (2012) 2662–2664.

[30] J.Y. Kwon, N.J. Singh, H.N. Kim, S.K. Kim, K.S. Kim, J. Yoon, Fluorescent GTP-sensing in aqueous solution of physiological pH, J. Am. Chem. Soc. 126 (2004) 8892–8893.

[31] G. Pratviel, B. Meunier, Guanine oxidation: one-and two-electron reactions, Chem. Eur. J. 12 (2006) 6018–6030.

[32] X.-.X. Wang, Q. Wu, Z. Shan, Q.-.M. Huang, BSA-stabilized Au clusters as peroxidase mimetics for use in xanthine detection, Biosens. Bioelectron. 26 (2011) 3614–3619.

[33] D. Kiga, Y. Futamura, K. Sakamoto, S. Yokoyama, An RNA aptamer to the xanthine/guanine base with a distinctive mode of purine recognition, Nucl. Acids Res. 26 (1998) 1755–1760.

[34] G. Connell, M. Yarus, RNAs with dual specificity and dual RNAs with similar specificity, Science 264 (1994) 1137–1141.

[35] M. Sassanfar, J.W. Szostak, An RNA motif that binds ATP, Nature 364 (1993) 550–553.

[36] R.D. Jenison, S.C. Gill, A. Pardi, B. Polisky, High-resolution molecular discrimination by RNA, Science 263 (1994) 1425–1429.

[37] A. Geiger, P. Burgstaller, H. Von der Eltz, A. Roeder, M. Famulok, RNA aptamers that bind L-arginine with sub-micromolar dissociation constants and high enantioselectivity, Nucl. Acids Res. 24 (1996) 1029–1036.

[38] P. Fan, A.K. Suri, R. Fiala, D. Live, D.J. Patel, Molecular recognition in the FMN–RNA aptamer complex, J. Mol. Biol. 258 (1996) 480–500.

[39] J.H. Davis, J.W. Szostak, Isolation of high-affinity GTP aptamers from partially structured RNA libraries, Proc. Natl. Acad. Sci. U. S. A. 99 (2002) 11616–11621.

[40] J.M. Carothers, S.C. Oestreich, J.H. Davis, J.W. Szostak, Informational complexity and functional activity of RNA structures, J. Am. Chem. Soc. 126 (2004) 5130–5137.

[41] J.M. Carothers, S.C. Oestreich, J.W. Szostak, Aptamers selected for higher-affinity binding are not more specific for the target ligand, J. Am. Chem. Soc. 128 (2006) 7929–7937.

[42] R. Nutiu, Y. Li, In vitro selection of structure-switching signaling atamers, Angew. Chem. Int. Ed. 44 (2005) 1061–1065.

[43] S.K. Silverman, DNA as a versatile chemical component for catalysis, encoding, and stereocontrol, Angew. Chem. Int. Ed. 49 (2010) 7180–7201.

[44] S.K. Silverman, Catalytic DNA: scope, applications, and biochemistry of deoxyribozymes, Trends Biochem. Sci. 41 (2016) 595–609.

[45] J. Liu, Z. Cao, Y. Lu, Functional nucleic acid sensors, Chem. Rev. 109 (2009) 1948–1998.

[46] D. Morrison, M. Rothenbroker, Y. Li, DNAzymes: selected for applications, Small Methods 2 (2018) 1700319.

[47] L. Ma, J. Liu, Catalytic nucleic acids: biochemistry, chemical biology, biosensors and nanotechnology, iScience 23 (2020) 100815.

[48] R.J. Lake, Z. Yang, J. Zhang, Y. Lu, DNAzymes as activity-based sensors for metal ions: recent applications, demonstrated advantages, current challenges, and future directions, Acc. Chem. Res. 52 (2019) 3275–3286.

[49] W. Zhou, R. Saran, J. Liu, Metal sensing by DNA, Chem. Rev. 117 (2017) 8272–8325.

[50] X.-.B. Zhang, R.-.M. Kong, Y. Lu, Metal ion sensors based on DNAzymes and related DNA molecules, Annu. Rev. Anal. Chem. 4 (2011) 105–128.

[51] W. Wang, L.P. Billen, Y. Li, Sequence diversity, metal specificity, and catalytic proficiency of metal-dependent phosphorylating DNA enzymes, Chem. Biol. 9 (2002) 507–517.

[52] S.A. McManus, Y. Li, Turning a kinase deoxyribozyme into a sensor, J. Am. Chem. Soc. 135 (2013) 7181–7186.

[53] L. Wang, Y. Liu, J. Li, Self-phosphorylating deoxyribozyme initiated cascade enzymatic amplification for guanosine-5′-triphosphate detection, Anal. Chem. 86 (2014) 7907–7912.

[54] W. Chiuman, Y. Li, Simple fluorescent sensors engineered with catalytic DNA 'MgZ'based on a non-classic allosteric design, PLoS ONE 2 (2007) e1224.

[55] L. Büttner, F. Javadi-Zarnaghi, C. Höbartner, Site-specific labeling of RNA at internal ribose hydroxyl groups: terbium-assisted deoxyribozymes at work, J. Am. Chem. Soc. 136 (2014) 8131–8137.

[56] Y. Wang, Z. Li, T.J. Weber, D. Hu, C.-.T. Lin, J. Li, et al., In situ live cell sensing of multiple nucleotides exploiting DNA/RNA aptamers and graphene oxide nanosheets, Anal. Chem. 85 (2013) 6775–6782.

[57] Y. Wang, L. Tang, Z. Li, Y. Lin, J. Li, In situ simultaneous monitoring of ATP and GTP using a graphene oxide nanosheet–based sensing platform in living cells, Nat. Protoc. 9 (2014) 1944.

[58] Y. Wang, Z. Li, D. Hu, C.-.T. Lin, J. Li, Y. Lin, Aptamer/graphene oxide nanocomplex for in situ molecular rrobing in living cells, J. Am. Chem. Soc. 132 (2010) 9274–9276.

[59] A. Serganov, D.J. Patel, Ribozymes, riboswitches and beyond: regulation of gene expression without proteins, Nat. Rev. Genet. 8 (2007) 776–790.

[60] M. Mandal, R.R. Breaker, Gene regulation by riboswitches, Nat. Rev. Mol. 5 (2004) 451–463.

[61] A. Serganov, E. Nudler, A decade of riboswitches, Cell 152 (2013) 17–24.

[62] B. Strobel, M. Spöring, H. Klein, D. Blazevic, W. Rust, S. Sayols, et al., High-throughput identification of synthetic riboswitches by barcode-free amplicon-sequencing in human cells, Nat. Commun. 11 (2020) 714.

[63] J. Noeske, C. Richter, M.A. Grundl, H.R. Nasiri, H. Schwalbe, J. Wohnert, An intermolecular base triple as the basis of ligand specificity and affinity in the guanine- and adenine-sensing riboswitch RNAs, Proc. Natl. Acad. Sci. U. S. A. 102 (2005) 1372–1377.

[64] M. Mandal, R.R. Breaker, Adenine riboswitches and gene activation by disruption of a transcription terminator, Nat. Struct. Mol. Biol. 11 (2004) 29–35.

[65] S. Findeiß, M. Etzel, S. Will, M. Mörl, P.F. Stadler, Design of artificial riboswitches as biosensors, Sensors 17 (2017) 1990.

[66] K.D. Smith, S.V. Lipchock, A.L. Livingston, C.A. Shanahan, S.A. Strobel, Structural and biochemical determinants of ligand binding by the c-di-GMP riboswitch, Biochemistry 49 (2010) 7351–7359.

[67] J.N. Kim, A. Roth, R.R. Breaker, Guanine riboswitch variants from Mesoplasma florum selectively recognize 2′-deoxyguanosine, Proc. Natl. Acad. Sci. U. S. A. 104 (2007) 16092–16097.

[68] O. Pikovskaya, A. Polonskaia, D.J. Patel, A. Serganov, Structural principles of nucleoside selectivity in a 2′-deoxyguanosine riboswitch, Nat. Chem. Biol. 7 (2011) 748.

[69] N. Kulshina, N.J. Baird, A.R. Ferré-D'Amaré, Recognition of the bacterial second messenger cyclic diguanylate by its cognate riboswitch, Nat. Struct. Mol. Biol. 16 (2009) 1212.

[70] N. Sudarsan, E. Lee, Z. Weinberg, R. Moy, J. Kim, K. Link, et al., Riboswitches in eubacteria sense the second messenger cyclic di-GMP, Science 321 (2008) 411–413.

[71] K.D. Smith, S.V. Lipchock, T.D. Ames, J. Wang, R.R. Breaker, S.A. Strobel, Structural basis of ligand binding by a c-di-GMP riboswitch, Nat. Struct. Mol. Biol. 16 (2009) 1218.

[72] C.A. Kellenberger, S.C. Wilson, J. Sales-Lee, M.C. Hammond, RNA-based fluorescent biosensors for live cell imaging of second messengers cyclic di-GMP and cyclic AMP-GMP, J. Am. Chem. Soc. 135 (2013) 4906–4909.

[73] S. Nakayama, Y. Luo, J. Zhou, T.K. Dayie, H.O. Sintim, Nanomolar fluorescent detection of c-di-GMP using a modular aptamer strategy, Chem. Comm. 48 (2012) 9059–9061.

[74] M. Tokui, T. Yamauchi, D. Miyoshi, H. Kamiya, A. Nishimura, N. Sugimoto, Rational design of a new IMP aptamer based on a TPP riboswitch and a hypoxanthine aptamer, Chem. Lett. 40 (2011) 1313–1314.

[75] Y. Li, J. Liu, Aptamer-based strategies for recognizing adenine, adenosine, ATP and related compounds, Analyst (2020), doi: 10.1039/D0AN00886A.

[76] L. Haase, B. Karg, K. Weisz, Manipulating DNA G−quadruplex structures by using guanosine analogues, ChemBioChem 20 (2019) 985–993.

[77] Q. Li, Y. Fei, L. Gao, Y. Yu, Y. Zhou, T. Ye, et al., G-quadruplex DNA with an apurinic site as a soft molecularly imprinted sensing platform, Anal. Chem. 90 (2018) 5552–5556.

[78] V. Esposito, L. Martino, G. Citarella, A. Virgilio, L. Mayol, C. Giancola, et al., Effects of abasic sites on structural, thermodynamic and kinetic properties of quadruplex structures, Nucl. Acids Res. 38 (2010) 2069–2080.

[79] J. Zhang, L.L. Wang, M.F. Hou, L.P. Luo, Y.J. Liao, Y.K. Xia, et al., Label-free fluorescent and electrochemical biosensors based on defective G-quadruplexes, Biosens. Bioelectron. 118 (2018) 1–8.

[80] J. Roy, P. Chirania, S. Ganguly, H. Huang, A DNA aptamer sensor for 8-oxo-7, 8-dihydroguanine, Bioorg. Med. Chem. Lett. 22 (2012) 863–867.

[81] M.K. Shigenaga, C.J. Gimeno, B.N. Ames, Urinary 8-hydroxy-2′-deoxyguanosine as a biological marker of in vivo oxidative DNA damage, Proc. Natl. Acad. Sci. U. S. A. 86 (1989) 9697–9701.

[82] X.m. Li, K.w. Zheng, Y.h. Hao, Z. Tan, Exceptionally selective and tunable sensing of guanine derivatives and analogues by structural complementation in a G-quadruplex, Angew. Chem. Int. Ed. 128 (2016) 13963–13968.

[83] K.-.B. Wang, J. Dickerhoff, G. Wu, D. Yang, PDGFR-β promoter forms a vacancy G-quadruplex that can be filled in by dGMP: solution structure and molecular recognition of guanine metabolites and drugs, J. Am. Chem. Soc. 142 (2020) 5204–5211.

[84] W. Zhou, J. Ding, J. Liu, A highly specific sodium aptamer probed by 2-aminopurine for robust Na^+ sensing, Nucl. Acids Res. 44 (2016) 10377–10385.

[85] W. Zhou, Y. Zhang, P.J. Huang, J. Ding, J. Liu, A DNAzyme requiring two different metal ions at two distinct sites, Nucl. Acids Res. 44 (2016) 354–363.

[86] Y. He, D. Chen, P.J. Huang, Y. Zhou, L. Ma, K. Xu, et al., Misfolding of a DNAzyme for ultrahigh sodium selectivity over potassium, Nucl. Acids Res. 46 (2018) 10262–10271.

[87] J. Hescheler, W. Rosenthal, W. Trautwein, G. Schultz, The GTP-binding protein, Go9 regulates neuronal calcium channels, Nature 325 (1987) 445–447.

[88] C. Kleuss, A.S. Raw, E. Lee, S.R. Sprang, A.G. Gilman, Mechanism of GTP hydrolysis by G-protein alpha subunits, Proc. Natl. Acad. Sci. U. S. A. 91 (1994) 9828–9831.

[89] T.C. Marlovits, W. Haase, C. Herrmann, S.G. Aller, V.M. Unger, The membrane protein FeoB contains an intramolecular G protein essential for Fe(II) uptake in bacteria, Proc. Natl. Acad. Sci. U. S. A. 99 (2002) 16243–16248.

[90] A. Bianchi-Smiraglia, M.S. Rana, C.E. Foley, L.M. Paul, B.C. Lipchick, S. Moparthy, et al., Internally ratiometric fluorescent sensors for evaluation of intracellular GTP levels and distribution, Nat. Methods 14 (2017) 1003.

[91] Q. Yin, Y. Tian, V. Kabaleeswaran, X. Jiang, D. Tu, M.J. Eck, et al., Cyclic di-GMP sensing via the innate immune signaling protein STING, Mol. Cell 46 (2012) 735–745.

[92] D.L. Burdette, K.M. Monroe, K. Sotelo-Troha, J.S. Iwig, B. Eckert, M. Hyodo, et al., STING is a direct innate immune sensor of cyclic di-GMP, Nature 478 (2011) 515–518.

[93] C. Shu, G. Yi, T. Watts, C.C. Kao, P. Li, Structure of STING bound to cyclic di-GMP reveals the mechanism of cyclic dinucleotide recognition by the immune system, Nat. Struct. Mol. Biol. 19 (2012) 722–724.

[94] G. Shang, D. Zhu, N. Li, J. Zhang, C. Zhu, D. Lu, et al., Crystal structures of STING protein reveal basis for recognition of cyclic di-GMP, Nat. Struct. Mol. Biol. 19 (2012) 725.

[95] Y.-.H. Huang, X.-.Y. Liu, X.-.X. Du, Z.-.F. Jiang, X.-.D. Su, The structural basis for the sensing and binding of cyclic di-GMP by STING, Nat. Struct. Mol. Biol. 19 (2012) 728.

[96] S. Nakayama, I. Kelsey, J. Wang, K. Roelofs, B. Stefane, Y. Luo, et al., Thiazole orange-induced c-di-GMP quadruplex formation facilitates a simple fluorescent detection of this ubiquitous biofilm regulating molecule, J. Am. Chem. Soc. 133 (2011) 4856–4864.

[97] Z. Zhang, S. Kim, B.L. Gaffney, R.A. Jones, Polymorphism of the signaling molecule c-di-GMP, J. Am. Chem. Soc. 128 (2006) 7015–7024.

[98] S. Kanvah, J. Joseph, G.B. Schuster, R.N. Barnett, C.L. Cleveland, U. Landman, Oxidation of DNA: damage to nucleobases, Acc. Chem. Res. 43 (2010) 280–287.

[99] V. Reipa, D.H. Atha, S.H. Coskun, C.M. Sims, B.C. Nelson, Controlled potential electro-oxidation of genomic DNA, PLoS ONE 13 (2018) e0190907.

[100] X. Wang, J. Zhang, Y. Wei, T. Xing, T. Cao, S. Wu, et al., Copper-based metal-organic framework/graphene nanocomposite for sensitive and stable electrochemical detection of DNA bases, Analyst 145 (2020) 1933–1942.

[101] T.S. Ortolani, T.S. Pereira, M.H. Assumpção, F.C. Vicentini, G.G. de Oliveira, B.C. Janegitz, Electrochemical sensing of purines guanine and adenine using single-walled carbon nanohorns and nanocellulose, Electrochim. Acta 298 (2019) 893–900.

[102] A.K. Geim, K.S. Novoselov, The rise of graphene, Nat. Mater. 6 (2010) 183–191.

[103] K.-.J. Huang, D.-.J. Niu, J.-.Y. Sun, C.-.H. Han, Z.-.W. Wu, Y.-.L. Li, et al., Novel electrochemical sensor based on functionalized graphene for simultaneous determination of adenine and guanine in DNA, Colloids Surf. B 82 (2011) 543–549.

[104] D. Wang, B. Huang, J. Liu, X. Guo, G. Abudukeyoumu, Y. Zhang, et al., A novel electrochemical sensor based on Cu@Ni/MWCNTs nanocomposite for simultaneous determination of guanine and adenine, Biosens. Bioelectron. 102 (2018) 389–395.

[105] D.R. Kumar, D. Manoj, J. Santhanalakshmi, Optimization of site specific adsorption of oleylamine capped CuO nanoparticles on MWCNTs for electrochemical determination of guanosine, Sens. Actuators B Chem. 188 (2013) 603–612.

[106] Q. Niu, C. Bao, X. Cao, C. Liu, H. Wang, W. Lu, Ni−Fe PBA hollow nanocubes as efficient electrode materials for highly sensitive detection of guanine and hydrogen peroxide in human whole saliva, Biosens. Bioelectron. 141 (2019) 111445.

[107] T. Yang, Q. Kong, Q. Li, X. Wang, L. Chen, K. Jiao, Highly sensitive and synergistic detection of guanine and adenine based on poly (xanthurenic acid)-reduced graphene oxide interface, ACS Appl. Mater. Interfaces 6 (2014) 11032–11037.

[108] M.M. Barsan, M.E. Ghica, C.M.A. Brett, Electrochemical sensors and biosensors based on redox polymer/carbon nanotube modified electrodes: a review, Anal. Chim. Acta 881 (2015) 1–23.

[109] G.D. Reid, D.J. Whittaker, M.A. Day, C.M. Creely, E.M. Tuite, J.M. Kelly, et al., Ultrafast electron-transfer reactions between thionine and guanosine bases, J. Am. Chem. Soc. 123 (2001) 6953–6954.

[110] T. Kulikova, A. Porfireva, G. Evtugyn, T. Hianik, Electrochemical DNA sensors with layered polyaniline-DNA coating for detection of specific DNA interactions, Sensors 19 (2019) 469.

[111] H. Liu, G. Wang, D. Chen, W. Zhang, C. Li, B. Fang, Fabrication of polythionine/NPAu/MWNTs modified electrode for simultaneous determination of adenine and guanine in DNA, Sens. Actuators B Chem. 128 (2008) 414–421.

[112] W. Yang, M. Ozsoz, D.B. Hibbert, J.J. Gooding, Evidence for the direct interaction between methylene blue and guanine bases using DNA-modified carbon paste electrodes, Electroanalysis 14 (2002) 1299–1302.

[113] X. Ba, L. Luo, Y. Ding, Z. Zhang, Y. Chu, B. Wang, et al., Poly(alizarin red)/graphene modified glassy carbon electrode for simultaneous determination of purine and pyrimidine, Anal. Chim. Acta 752 (2012) 94–100.

[114] Y.-.S. Gao, J.-.K. Xu, L.-.M. Lu, L.-.P. Wu, K.-.X. Zhang, T. Nie, et al., Overoxidized polypyrrole/graphene nanocomposite with good electrochemical performance as novel electrode material for the detection of adenine and guanine, Biosens. Bioelectron. 62 (2014) 261–267.

[115] X. Liu, L. Zhang, S. Wei, S. Chen, X. Ou, Q. Lu, Overoxidized polyimidazole/graphene oxide copolymer modified electrode for the simultaneous determination of ascorbic acid, dopamine, uric acid, guanine and adenine, Biosens. Bioelectron. 57 (2014) 232–238.

[116] X. Xu, L. He, Y. Long, S. Pan, H. Liu, J. Yang, et al., S-doped carbon dots capped ZnCdTe quantum dots for ratiometric fluorescence sensing of guanine, Sens. Actuators B Chem. 279 (2019) 44–52.

[117] L. Fu, L. Yan, G. Wang, H. Ren, L. Jin, Photoluminescence enhancement of silver nanoclusters assembled on the layered double hydroxides and their application to guanine detection, Talanta 193 (2019) 161–167.

[118] S. Wang, C. Liu, G. Li, Y. Sheng, Y. Sun, H. Rui, et al., The triple roles of glutathione for a DNA-cleaving DNAzyme and development of a fluorescent glutathione/Cu^{2+}-dependent DNAzyme sensor for detection of Cu^{2+} in drinking water, ACS Sens. 2 (2017) 364–370.

[119] Y.-.J. Tong, L.-.D. Yu, L.-.L. Wu, S.-.P. Cao, Y.-.L. Guo, R.-.P. Liang, et al., Ratiometric detection of Cu^{2+} using a luminol-Tb-GMP nanoprobe with high sensitivity and selectivity, ACS Sustain. Chem. Eng. 6 (2018) 9333–9341.

[120] B. Liu, H. Shen, D. Liu, Y. Hao, X. Zhu, Q. Shen, et al., Citrate/Tb lanthanide coordination polymer nanoparticles: preparation and sensing of guanosine-5-monophosphate, Sens. Actuators B Chem. 300 (2019) 126879.

[121] N.T.K. Thanh, D.L. Rathbone, D.C. Billington, N.A. Hartell, Selective recognition of cyclic GMP using a fluorescence-based molecularly imprinted polymer, Anal. Lett. 35 (2002) 2499–2509.
[122] Z. Zhang, J. Liu, Molecular imprinting with functional DNA, Small 15 (2019) 1805246.
[123] Z. Zhang, J. Liu, Molecularly imprinted polymers with DNA aptamer fragments as macromonomers, ACS Appl. Mater. Interfaces 8 (2016) 6371–6378.
[124] J. Wu, X. Wang, Q. Wang, Z. Lou, S. Li, Y. Zhu, et al., Nanomaterials with enzyme-like characteristics (nanozymes): next-generation artificial enzymes (II), Chem. Soc. Rev. 48 (2019) 1004–1076.
[125] Y. Huang, J. Ren, X. Qu, Nanozymes: classification, catalytic mechanisms, activity regulation, and applications, Chem. Rev. 119 (2019) 4357–4412.
[126] Y. Zhou, B. Liu, R. Yang, J. Liu, Filling in the gaps between nanozymes and enzymes: challenges and opportunities, Bioconjug. Chem. 28 (2017) 2903–2909.